

Available online at [www.sciencedirect.com](http://www.sciencedirect.com)

SCIENCE @ DIRECT®

Life Sciences xx (2006) xxx–xxx

*Life Sciences*[www.elsevier.com/locate/lifescie](http://www.elsevier.com/locate/lifescie)

## Age-related decline of dopamine synthesis in the living human brain measured by positron emission tomography with L-[ $\beta$ - $^{11}\text{C}$ ]DOPA

Miho Ota <sup>a,b</sup>, Fumihiko Yasuno <sup>a</sup>, Hiroshi Ito <sup>a,\*</sup>, Chie Seki <sup>a</sup>, Shoko Nozaki <sup>a</sup>,  
Takashi Asada <sup>c</sup>, Tetsuya Suhara <sup>a</sup>

<sup>a</sup> *Clinical Neuroimaging Section, Department of Molecular Neuroimaging, Molecular Imaging Center, National Institute of Radiological Sciences, 4-9-1 Anagawa, Inage-ku, Chiba 263-8555, Japan*

<sup>b</sup> *Comprehensive Human Sciences, Medical Sciences for Control of Pathological Processes, Clinical Neuroscience, University of Tsukuba Graduate School, Tsukuba, Japan*

<sup>c</sup> *Department of Psychiatry, University of Tsukuba, Tsukuba, Japan*

Received 5 December 2005; accepted 15 February 2006

### Abstract

Loss of dopamine synthesis in the striatum with normal human aging has been observed in the postmortem brain. To investigate whether there is age-associated change in dopamine synthesis in the extrastriatal brain regions similar to that in the striatum, positron emission tomography studies with  $^{11}\text{C}$ -labelled L-DOPA were performed on 21 normal healthy male subjects (age range 20–67 years). Decline in the tissue fraction of gray matter per region of interest was also investigated. The overall uptake rate constant for each region of interest was quantified by the Patlak plot method using the occipital cortex as reference region. Regions of interest were set on the dorsolateral prefrontal cortex, lateral temporal cortex, medial temporal cortex, occipital cortex, parietal cortex, anterior cingulate, thalamus, midbrain, caudate nucleus, and putamen. Test–retest analysis indicated good reproducibility of the overall uptake rate constant. Significant age-related declines of dopamine synthesis were observed in the striatum and extrastriatal regions except midbrain. The decline in the overall uptake rate constant was more prominent than in the tissue fraction of gray matter. These results indicate that the previously demonstrated age-related decline in striatal dopamine synthesis extends to several extrastriatal regions in normal human brain.

© 2006 Elsevier Inc. All rights reserved.

**Keywords:** Aging; Reproducibility; L-[ $\beta$ - $^{11}\text{C}$ ]DOPA; Positron emission tomography

### Introduction

Morphological and neurochemical changes are believed to take place in the human central nervous system during the aging process, which might lead to increased vulnerability to the development of several physiological disturbances and neuro-psychiatric disorders closely related to age (Arranz et al., 1996). Postmortem studies indicated that the level of dopamine synthesis (Kish et al., 1992) and several other endogenous neurotransmitters declines in the human striatum during aging (Kish et al., 1995). To estimate the changes of

extrastriatal dopamine synthesis in vivo in the living human brain, positron emission tomography (PET) can be used. The ligand  $^{11}\text{C}$ -labelled L-DOPA in the carboxy group (L-[ $\beta$ - $^{11}\text{C}$ ]DOPA) has been reported to be useful for the quantification of L-DOPA metabolism in the brain (Tedroff et al., 1992). Labeling of L-DOPA with  $^{11}\text{C}$  allows study with a molecule identical to endogenous L-DOPA as a tracer. In the present study, we evaluated the reproducibility of PET measurement with L-[ $\beta$ - $^{11}\text{C}$ ]DOPA and age-related changes in dopamine synthesis.

It is also known from postmortem and in vivo studies that the brain shrinks with age (Good et al., 2001). To compare the change of dopamine synthesis with aging in the cerebral cortices, we also investigated age-related atrophy of cerebral cortices using images of gray matter fraction derived from magnetic resonance imaging (MRI).

\* Corresponding author. Tel.: +81 43 206 4702; fax: +81 43 253 0396.  
E-mail address: [hito@nirs.go.jp](mailto:hito@nirs.go.jp) (H. Ito).

## Materials and methods

### Subjects

Twenty-one healthy male volunteers, age 20 to 67 years ( $40.0 \pm 15.7$ , mean  $\pm$  SD), participated in the study, and 7 of them, age 20 to 26 years ( $22.3 \pm 2.1$ ), twice underwent PET scans to assess reproducibility. They had no medical history and no brain abnormalities when examined by MRI. This study was approved by the Ethics and Radiation Safety Committees of the National Institute of Radiological Sciences, Chiba, Japan. All participants gave their written informed consent.

### Positron emission tomography study

PET scans were performed using an ECAT EXACT HR+ system (CTI-Siemens, Knoxville, Tennessee, USA) in three-dimensional mode, which provides 63 planes and a 15.5 cm field of view. L-[ $\beta$ - $^{11}\text{C}$ ]DOPA was synthesized from [ $^{11}\text{C}$ ] carbon dioxide via D,L-[ $3$ - $^{11}\text{C}$ ]alanine as described previously (Bjurling et al., 1990; Sasaki et al., 2000). After a 10-min transmission scan with a  $^{68}\text{Ge}$ – $^{68}\text{Ga}$  source, a bolus of 258–392 MBq of L-[ $\beta$ - $^{11}\text{C}$ ]DOPA was injected with specific radioactivity of 12.2 GBq/ $\mu\text{mol}$  to 81.1 GBq/ $\mu\text{mol}$  at the time of injection into the antecubital vein with a 20-ml saline flush. Dynamic PET scanning was started simultaneously with the tracer injection and continued for 60 min (Gefvert et al., 2003). Twenty-three time frames (length: 0.5, 1, 2, 3, 4, or 5 min) were collected. All emission scans were reconstructed with a Hanning filter with a cut-off frequency of 0.4 (full width at half maximum (FWHM)=7.5 mm).

Regions of interest (ROIs) were placed manually on 10 regions (dorsolateral prefrontal cortex, lateral temporal cortex, medial temporal cortex, occipital cortex, parietal cortex, anterior cingulate, thalamus, midbrain, caudate nucleus, and putamen) of the T1-weighted image that had been resliced and coregistered to the PET summation image (0–60 min) individually using SPM2 (Friston et al., 1995). Brain structures were also ascertained by human brain atlas (Mai et al., 1997). Then, time–activity curves of the 10 brain regions were obtained.

For test–retest analysis, seven subjects each underwent two PET scans. The intervals between the test and retest scans were 3 weeks or less. Since it is known that dopamine activity in plasma follows a circadian rhythm (Markianos and Lykouras, 1981), the test–retest studies were performed at the same time of the day.

### Magnetic resonance imaging study

T1-weighted images of the brain were obtained from all subjects with a Philips Intera, 1.5 T (Philips Medical Systems, Best, The Netherlands). Scan parameters were 1-mm thick 3 D T1 images with a transverse plane (repetition time, TR/echo time, TE 21/9.2 ms, flip angle 30°, matrix 256  $\times$  256, field of view (FOV) 256  $\times$  256), yielding 196 contiguous slices through the head.

### PET data analysis

The overall uptake rate constant ( $K$ ) that quantifies dopamine synthesis was calculated using the graphical analysis developed by Patlak et al. (Patlak and Blasberg, 1985). This analytical method was developed for irreversible ligands and allows for the calculation of  $K$  using time–activity data in a reference brain region with no irreversible binding.  $K$  values can be estimated by simple linear least squares fitting as follows:

$$\frac{C_i(t)}{C_i'(t)} = K \frac{\int_0^t C_i'(\tau) d\tau}{C_i'(t)} + F_{D,t^*}$$

where  $C_i$  is the total radioactivity concentration in a brain region, which can be measured by PET;  $C_i'$  is the total radioactivity concentration in a brain region with no irreversible compartments;  $t^*$  is the equilibrium time of the compartment for unchanged radioligand in the brain tissue. Plotting  $C_i(t)/C_i'(t)$  versus  $\int_0^t C_i'(\tau) d\tau/C_i'(t)$ , after a time  $t^*$  yields a straight line with the slope  $K$  and intercept  $F$ . In the present study, the occipital cortex was used as a region with no irreversible compartments (Torstenson et al., 1997). A range of equilibrium time  $t^*$  of 31.5 to 61.5 min was used.

### MRI data analysis

Gray matter, white matter, and cerebrospinal fluid images were segmented and extracted from registered MR images using SPM99 (Friston et al., 1995). These segmented MR images provide the tissue fractions of gray and white matter and fraction of cerebrospinal fluid per pixel (ml/ml) (Ito et al., 2005). All gray matter images were smoothed with an isotropic Gaussian kernel at 8-mm FWHM, the same as the FWHM of the PET scanner. Gray matter fraction was obtained from tissue fraction images of gray matter. ROIs used for PET data analysis were drawn on the tissue fraction image of gray matter. ROIs were defined for the dorsolateral prefrontal, lateral temporal, parietal, occipital cortices, anterior cingulate and medial temporal cortex.

### Statistics

Statistical analyses were performed with SPSS for Windows 11.0.1.j (SPSS Inc, 1989–2001). The relationship between age and  $K$  was evaluated by Pearson's correlation method. For correlation analysis, a  $p$  value  $< 0.005$  ( $= 0.05/9$ ) was considered significant to avoid type errors in the multiplicity of statistical analysis. The relationship between age and tissue fractions of gray matter was also evaluated by Pearson's correlation method. For correlation analysis, a  $p$  value  $< 0.017$  ( $0.05/3$ ) was considered significant.

Reproducibility was assessed in terms of variability and reliability. Within-subject variability was defined as the absolute value of the difference between the test and retest

Table 1  
Reproducibility of 11 C-labelled L-DOPA  $K$  values in human brain

	DorFro	Tempo	Parie	Mid	Med Temp	ACing	Thal	Cau	Puta
Test $K$ ( $\text{min}^{-1}$ ) (mean $\pm$ S.D.) $\times e^3$	2.7 $\pm$ 0.3	3.4 $\pm$ 0.5	2.1 $\pm$ 0.5	60.4 $\pm$ 0.9	5.7 $\pm$ 0.4	4.6 $\pm$ 0.6	4.9 $\pm$ 0.9	14.6 $\pm$ 1.7	16.6 $\pm$ 0.7
Retest $K$ ( $\text{min}^{-1}$ ) (mean $\pm$ S.D.) $\times e^3$	2.6 $\pm$ 0.5	3.1 $\pm$ 0.5	2.0 $\pm$ 0.4	6.0 $\pm$ 1.0	5.7 $\pm$ 0.7	4.6 $\pm$ 0.6	4.7 $\pm$ 1.0	14.1 $\pm$ 1.8	16.5 $\pm$ 1.8
Variability	9.4 $\pm$ 8.6	10.1 $\pm$ 6.3	10.1 $\pm$ 6.3	9.2 $\pm$ 9.6	8.8 $\pm$ 4.1	9.3 $\pm$ 7.3	8.8 $\pm$ 5.2	7.3 $\pm$ 6.5	7.3 $\pm$ 2.4
ICC	0.78	0.76	0.87	0.71	0.54	0.58	0.90	0.73	0.51

DorFro, dorsolateral prefrontal cortex; Tempo, lateral temporal cortex; Parie, parietal cortex; Mid, midbrain; Med Temp, medial temporal cortex; ACing, anterior cingulate; Thal, thalamus; Cau, caudate nucleus; Puta, putamen.

measurements expressed as the percentage of the mean value of the two measurements.

$$\text{Variability}(\%) = (\text{test} - \text{retest}) \times 100 / \{(\text{test} + \text{retest}) / 2\}$$

A measure of the reliability was assessed with the intraclass correlation coefficient (ICC) according to the following equation:

$$\text{ICC} = (\text{MSBS} - \text{MSWS}) / (\text{MSBS} + [n - 1]\text{MSWS})$$

where MSBS is the mean sum of squares between subjects, MSWS is the mean sum of squares within subjects, and  $n$  is the number of repeated observations (in this case,  $n=2$ ). This coefficient is an estimate of the reliability of the two sets of measurement and varies from  $-1$  (not reliable) to  $+1$  (perfectly reliable, i.e., identical test and retest measurements).

To confirm that the shape of the time–activity curve in the occipital cortex used as reference region was unchanged during aging, repeated measures ANOVA was performed for time–activity curves in the occipital cortex normalized by the radioactivity injected and the subject's weight.

## Results

Test–retest results are summarized in Table 1. The uptake of  $^{11}\text{C}$ -labelled L-DOPA was highest in the putamen. Among the extrastriatal regions,  $K$  value was highest in the midbrain (mean  $K=0.0062$ ) and lowest in the parietal cortex (0.0020). All  $K$  value measurements showed good to excellent reproducibility with high intraclass correlation coefficients (0.51–0.90) and small within-subject variability with no systematic differences in  $K$  values between test and retest (7.3–10.3%).

Repeated measures ANOVA was used to compare radioactivity of the occipital cortex, adjusted for injected dose and weight, among 5 different generation groups (20–29 years old,

30–39, 40–49, 50–59, 60–67) across the 4 frames (31.5, 41.5, 51.5, 61.5 min). There was no significant interaction of group  $\times$  frame ( $F_{12, 48}=0.45$ ;  $p=0.94$ ). Time–activity curves in the occipital cortex did not differ significantly according to age.

The  $K$  value of L- $[\beta\text{-}^{11}\text{C}]\text{DOPA}$  showed a significant negative correlation with age in the dorsolateral prefrontal cortex, lateral temporal cortex, parietal cortex, anterior cingulate, thalamus, medial temporal cortex, caudate nucleus, and putamen, but not in the midbrain (Table 2 and Fig. 1). When linear regression was applied to fit the data, the decrease in  $K$  was 16.4% per decade in the dorsolateral prefrontal cortex, 13.8% in lateral temporal cortex, 16.2% in parietal cortex, 8.4% in medial temporal cortex, 13.7% in anterior cingulate, 10.7% in thalamus, 5.4% in caudate nucleus, and 4.2% in putamen.

The tissue fractions of gray matter showed significant negative correlations with age in the cerebral cortex and anterior cingulate (Table 3), with decreases of 3.2% and 2.8% per decade, respectively.

## Discussion

We demonstrated very small within-subject variability and high ICC. ROI-based analysis revealed variability of 7.3–10.1% and ICC of 0.51–0.90 for the regions. ICC has often been used as a measure of reliability, with values between 0.4 and 0.75 regarded as fair to good reliability, and greater than 0.9 as excellent (Fleiss, 1986). This criterion also supports the accuracy of the test–retest reliability of L- $[\beta\text{-}^{11}\text{C}]\text{DOPA}$  measurement of these regions. Regional distribution of  $K$  value in the brain also corresponds well with postmortem studies of the distribution of aromatic L-amino acid decarboxylase (AADC) (Lloyd and Hornykiewicz, 1972).

In the human brain, significant losses over a normal life span have been reported for dopamine transporters (Volkow

Table 2  
Associations of age and  $K$  analyzed using Pearson's correlation coefficients

	DorFro	Tempo	Parie	Mid	Med Temp	ACing	Thal	Cau	Puta
Correlation coefficients	–0.75	–0.65	–0.69	–0.24	–0.69	–0.65	–0.62	–0.60	–0.62
$p$ value	<0.001	0.002	<0.001	0.289	0.001	0.001	0.003	0.004	0.003

DorFro, dorsolateral prefrontal cortex; Tempo, lateral temporal cortex; Parie, parietal cortex; Mid, midbrain; Med Temp, medial temporal cortex; ACing, anterior cingulate; Thal, thalamus; Cau, caudate nucleus; Puta, putamen.

et al., 1996), dopamine D<sub>2</sub> receptors (Kaasinen et al., 2000; Inoue et al., 2001), and dopamine D<sub>1</sub> receptors (Suhara et al., 1991). The results of studies on age-related change of dopamine synthesis have been less consistent, showing decreases (Martin et al., 1989) as well as no changes with aging (Eidelberg et al., 1993; Sawle et al., 1990; Laakso et al., 2001) by PET using 6-[<sup>18</sup>F]fluoro-L-DOPA. However, previous postmortem studies have reported remarkable age-dependent decreases in the striatal activity of dopa decarboxylase (Lloyd and Hornykiewicz, 1972; Kish et al., 1995). Our study with L-[β-<sup>11</sup>C]DOPA showed that dopamine synthesis not only in the striatum but also in extrastriatal regions of the living human brain decreased with the normal aging process. 3-*O*-Methyl-L-DOPA, a metabolite of L-DOPA, is known to pass the blood-brain barrier (Wade and Katzman, 1975). In previous PET studies using 6-[<sup>18</sup>F]fluoro-L-DOPA, dopamine synthesis was affected by 6-[<sup>18</sup>F]fluoro-3-*O*-methyl-L-DOPA in the brain (Kuwabara et al., 1993; Dhawan et al., 1996). However, nevertheless the 6-[<sup>18</sup>F]fluoro-3-*O*-methyl-L-DOPA concentrations in the plasma and cerebellum were greater in the elderly group (Kumakura et al., 2005), the time-activity

curve of L-[β-<sup>11</sup>C]DOPA in the occipital, which was used as the reference region did not change with aging in this study. It is also known that 3-*O*-Methylation of 6-fluoro-L-DOPA takes place rapidly as compared to L-DOPA (Torstenson et al., 1999; Melega et al., 1990). The difference between previous results using 6-[<sup>18</sup>F]fluoro-L-DOPA and ours using L-[β-<sup>11</sup>C]DOPA may be due to metabolism differences in plasma and brain between the two ligands.

Neutral amino acids are transported from the blood to the brain using the same carrier system in a competitive fashion (Oldendorf, 1971). L-DOPA is also mediated by the same carrier system. *K* consists of *K*<sub>1</sub>, which represents the influx rate of L-[β-<sup>11</sup>C]DOPA across the blood-brain barrier, and *k*<sub>3</sub>, which represents the rate of activity of AADC to catabolize L-DOPA to dopamine (Patlak and Blasberg, 1985). L-[β-<sup>11</sup>C]DOPA is transported in a competitive fashion with neutral amino acids. But it was shown that there was no significant decline in neutral amino acid transport with the carrier system with age (Koeppel et al., 1990; Ito et al., 1995).

*K*<sub>1</sub> values of L-[β-<sup>11</sup>C]DOPA were very small (data not shown), indicating that small PS (capillary permeability-

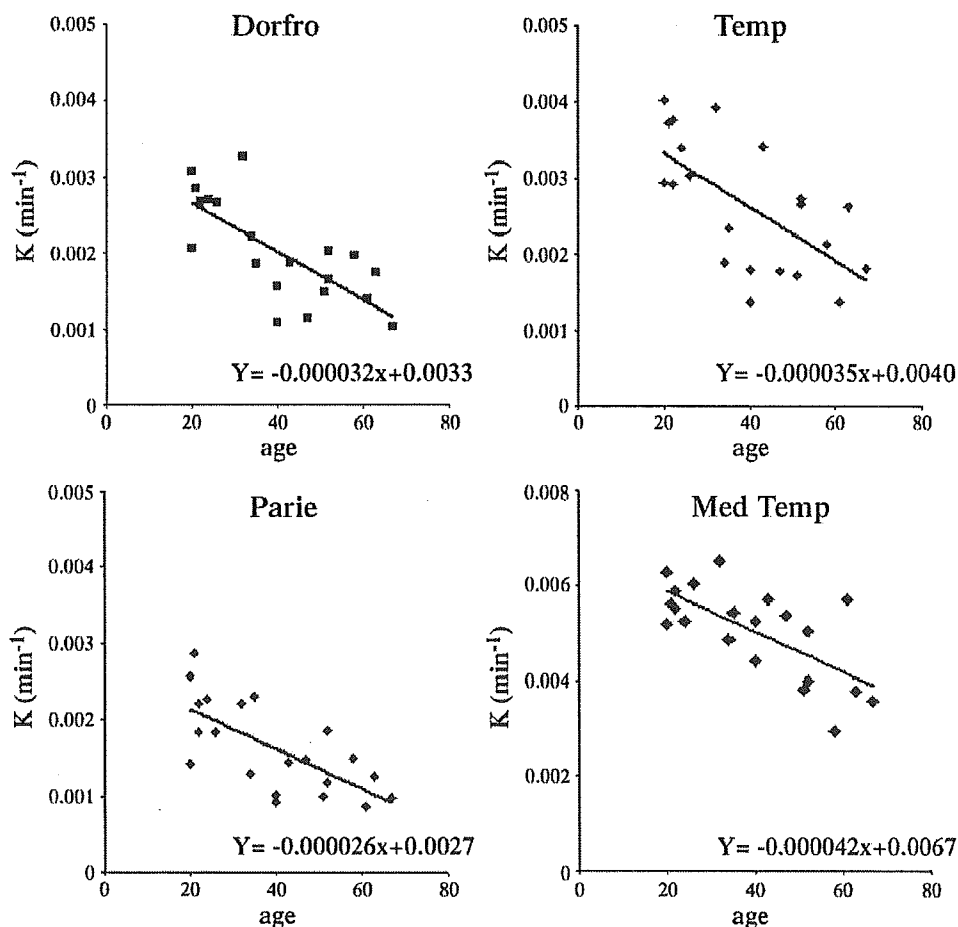


Fig. 1. *K* of L-[β-<sup>11</sup>C]DOPA plotted against age in ROI. In the regression equation, 'Y' corresponds to *K* and 'x' corresponds to age. DorFro, dorsolateral prefrontal cortex; Tempo, lateral temporal cortex; Parie, parietal cortex; Mid, midbrain; Med Tem, medial temporal cortex; ACing, anterior cingulate; Thal, thalamus; Cau, caudate nucleus; Puta, putamen.

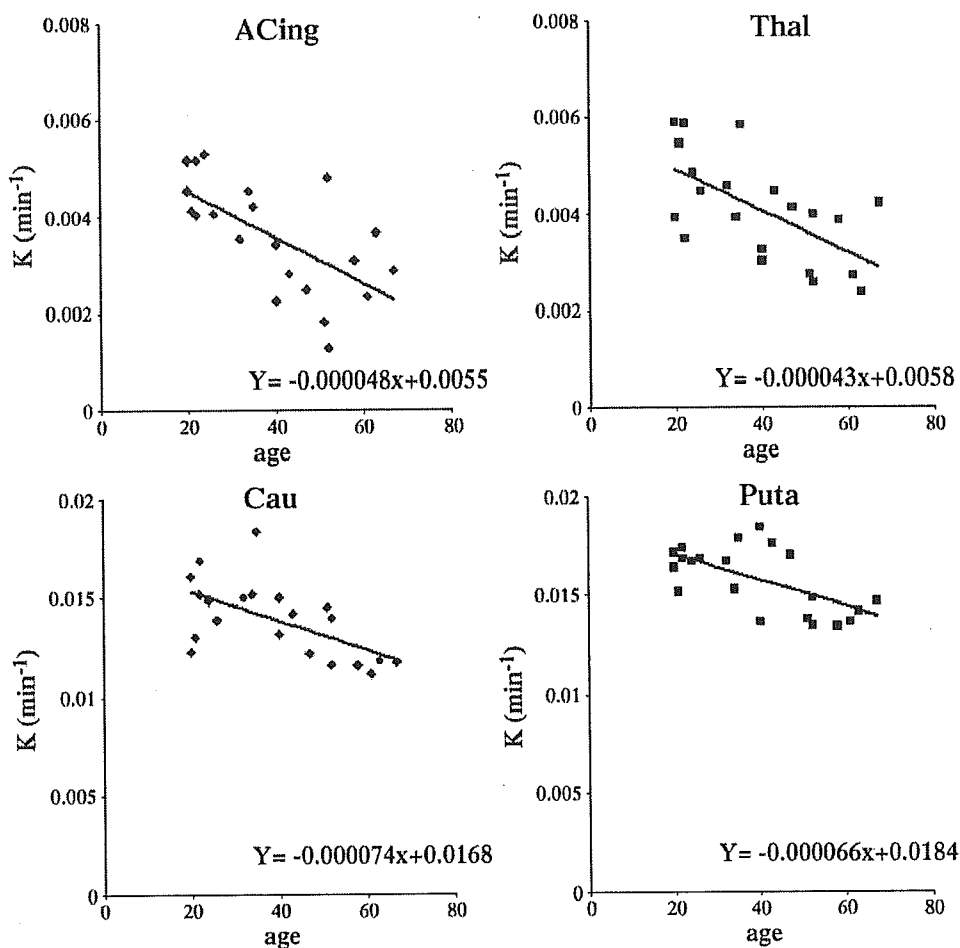


Fig. 1 (continued).

surface area product) values, such as  $K_1$  values of L-[ $\beta$ -<sup>11</sup>C] DOPA, are independent of regional cerebral blood flow (Crone, 1963; Renkin, 1959). With this ligand, graphical analysis using a reference brain region can be used even if the cerebral blood flow changes in a brain region as compared to a reference brain region. Thus, the effect of aging on the  $K$  value of L-[ $\beta$ -<sup>11</sup>C]DOPA must represent the aging effect on dopamine synthesis.

The present study focused on the age-related change in dopamine synthesis. PET studies concerning the aging effect of the striatal dopaminergic neurotransmitter system have shown 6–8% decrease of  $D_2$  receptor binding potential per decade of life (Kaasinen et al., 2000), 6.9% decrease of  $D_1$  receptor binding in the caudate and 7.4% in the putamen per decade (Wang et al., 1998), 8.0% decrease of  $D_1$  receptor binding in the striatum per decade (Suhara et al., 1991), 7.3% decrease of dopamine transporter in caudate nucleus and 5.2% in the putamen per decade (Tupala et al., 2003), and 27% decrease of dopa decarboxylase per 50 years in the postmortem caudate nucleus (Kish et al., 1995). The same magnitude of decline of striatal  $K$  was observed in the present study, suggesting a striatal pre- and postsynaptic

dopaminergic neurotransmitter system decrease of about 6% per decade. PET studies have also shown a 6% decrease of binding potential of vesicular monoamine transporter, type 2 in the striatum per decade of life (Taylor et al., 2000) and shown the age-related decline in the capacity for [<sup>18</sup>F] fluorodopamine retention in the striatum (Kumakura et al., 2005). These results were in good agreement with our suggestion. Our study also showed that the rate of dopamine synthesis decline was faster in extrastriatal regions than in the striatum, and especially faster in the dorsolateral prefrontal cortex as compared to the other regions. This result is compatible with the studies of  $D_1$  and  $D_2$  receptors (Suhara et al., 1991; Kaasinen et al., 2000). The dorsolateral

Table 3  
Associations of age and tissue fraction of gray matter analyzed using Pearson's correlation coefficients

	Cortex	Med Temp	ACing
Correlation coefficients	-0.777	-0.331	-0.593
$p$ value	0.000	0.142	0.005

Med Temp, medial temporal cortex; ACing, anterior cingulate.

prefrontal cortex is the crucial locus for dopaminergic effects on high-level cognitive functions such as planning, spatial working memory, attention, measure of abstraction, mental flexibility, and verbal fluency (Cools et al., 2002). It is known that the decline in brain dopamine activity contributes to impaired performance of tasks involving the dorsolateral prefrontal regions (Gotham et al., 1988; Owen et al., 1992; Volkow et al., 1998). Our study may suggest that the decline of dopamine synthesis in the dorsolateral prefrontal cortex could explain the decline of cognitive performance with aging. Concerning the lack of aging effect in the midbrain, this region includes the substantia nigra where dopamine is well synthesized. However, the substantia nigra itself is too small in volume to allow accurate quantification of  $K$ .

As compared with the aging effects of  $K$ , a decline in the tissue fraction of gray matter was found in the cerebral cortex. It is known that volume loss during aging occurs in the cerebral cortex (Taki et al., 2004). Furthermore, areas of relative preservation of gray matter volume were noted symmetrically in the lateral thalami, amygdala, hippocampi, and entorhinal cortex (Good et al., 2001). Our observation is consistent with these results. The degree of decrease in the tissue fraction of gray matter in the cerebral cortical region was smaller than that of the previous report (Taki et al., 2004). This may be due to the fact that the loss of gray matter tissue fraction accelerates through the course of life, and particularly at advanced age, and our subjects were relatively younger than those of the previous study, in which 16–79-year-old subjects participated. In the present study, the decline in cortical  $K$  was faster and more diffusely distributed than that of gray matter volume. This may indicate that the dopaminergic function decreases faster than morphological changes.

In this study, we evaluate only in males. Numerous gender-associated functional, biological differences in the dopamine systems of the brain have been described (Kaasinen et al., 2001). Further works concerning sex difference of the dopamine system using the same method will be necessary.

## Conclusion

We confirmed the reproducibility of L- $[\beta\text{-}^{11}\text{C}]\text{DOPA}$  quantification. Significant age-related declines of dopamine synthesis in the striatum and extrastriatal regions were observed, indicating that the previously demonstrated age-related decline in the striatal dopamine synthesis extends to several extrastriatal regions in normal human males. Our results also showed that the rate of dopamine synthesis decline was the same magnitude as the loss of dopamine  $D_1$  and  $D_2$  receptors and transporters.

## Acknowledgements

We wish to extend our gratitude to Mr. Katsuyuki Tanimoto, Mr. Akira Ando, Mr. Takahiro Shiraiishi, and Mr. Masaru Ohno for operation of the PET scanner, and to Mr. Kazutoshi Suzuki,

cyclotron personnel, for synthesizing the radioligand. We also gratefully acknowledge Drs. Jun Kosaka, Yota Fujimura, Akihiro Takano, and Ms Yoshiko Fukushima for their helpful discussions and PET data acquisition. This research was supported by grants from the National Institute of Radiological Sciences.

## References

- Arranz, B., Blennow, K., Ekman, R., Eriksson, A., Mansson, J.E., Marcusson, J., 1996. Brain monoaminergic and neuropeptidergic variations in human aging. *Journal of Neural Transmission* 103, 101–115.
- Bjurling, P., Watanabe, Y., Oka, S., Nagasawa, T., Yamada, H., Langstrom, B., 1990. Multi-enzymatic syntheses of beta- $^{11}\text{C}$ -labeled L-tyrosine and L-DOPA. *Acta Chemica Scandinavica* 44, 183–188.
- Cools, R., Stefanova, E., Barker, R.A., Robbins, T.W., Owen, A.M., 2002. Dopaminergic modulation of high-level cognition in Parkinson's disease: the role of the prefrontal cortex revealed by PET. *Brain* 125 (Pt 3), 584–594.
- Crone, C., 1963. Permeability of capillaries in various organs as determined by use of the indicator diffusion method. *Acta Physiologica Scandinavica* 58, 292–305.
- Dhawan, V., Ishikawa, T., Patlak, C., Chaly, T., Robeson, W., Belakhlef, A., Margouleff, C., Mandel, F., Eidelberg, D., 1996. Combined FDOPA and 3OMFD PET studies in Parkinson's disease. *Journal of Nuclear Medicine* 37, 209–216.
- Eidelberg, D., Takikawa, S., Dhawan, V., Chaly, T., Robeson, W., Dahl, R., Margouleff, D., Moeller, J.R., Patlak, C.S., Fahn, S., 1993. Striatal  $^{18}\text{F}$ -DOPA uptake: absence of an aging effect. *Journal of Cerebral Blood Flow and Metabolism* 13, 881–888.
- Fleiss, J., 1986. *The Design and Analysis of Clinical Experiments*. John Wiley and Sons, New York.
- Friston, K.J., Holmes, A.P., Worsley, K.J., Poline, J.B., Frith, C., Frackowiak, R., 1995. Statistical parametric maps in functional imaging: a general linear approach. *Human Brain Mapping* 2, 189–210.
- Gefvert, O., Lindstrom, L.H., Waters, N., Waters, S., Carlsson, A., Tedroff, J., 2003. Different corticostriatal patterns of L-DOPA utilization in patients with untreated schizophrenia and patients treated with classical antipsychotics or clozapine. *Scandinavian Journal of Psychology* 44 (3), 289–292.
- Good, C.D., Johnsrude, I.S., Ashburner, J., Henson, R.N.A., Friston, K.J., Frackowiak, R.S.J., 2001. A voxel-based morphometric study of aging in 465 normal adult human brains. *Neuroimage* 14, 21–36.
- Gotham, A.M., Brown, R.G., Marsden, C.D., 1988. 'Frontal' cognitive function in patients with Parkinson's disease 'on' and 'off' levodopa. *Brain* 111 (Pt 2), 299–321.
- Inoue, M., Suhara, T., Sudo, Y., Okubo, Y., Yasuno, F., Kishimoto, T., Yoshikawa, K., Tanada, S., 2001. Age-related reduction of extrastriatal dopamine D2 receptor measured by PET. *Life Sciences* 69, 1079–1084.
- Ito, H., Hatazawa, J., Murakami, M., Miura, S., Iida, H., Bloomfield, P.M., Kanno, I., Fukuda, H., Uemura, K., 1995. Aging effect on neutral amino acid transport at the blood-brain barrier measured with L- $[2\text{-}^{18}\text{F}]\text{-fluorophenylalanine}$  and PET. *Journal of Nuclear Medicine* 36, 1232–1237.
- Ito, H., Shidahara, M., Inoue, K., Goto, R., Kinomura, S., Taki, Y., Okada, K., Kaneta, T., Sato, K., Sato, T., Fukuda, H., 2005. Effects of tissue heterogeneity on cerebral vascular response to acetazolamide stress measured by an I-123 IMP autoradiographic method with single-photon emission computed tomography. *Annals of Nuclear Medicine* 19 (4), 251–260.
- Kaasinen, V., Vilkinen, H., Hietala, J., Nagren, K., Helenius, H., Olsson, H., Farde, L., Rinne, J.O., 2000. Age-related dopamine D2/D3 receptor loss in extrastriatal regions of the human brain. *Neurobiology of Aging* 21 (5), 683–688.
- Kaasinen, V., Nagren, K., Hietala, J., Farde, L., Rinne, J.O., 2001. Sex differences in extrastriatal dopamine d(2)-like receptors in the human brain. *American Journal of Psychiatry* 158, 308–311.
- Kish, S.J., Shannak, K., Rajput, A., 1992. Aging produced a specific pattern of striatal dopamine loss: implication for the etiology of idiopathic Parkinson's disease. *Journal of Neurochemistry* 58, 642–648.

- Kish, S.J., Zhong, X.H., Hornykiewicz, O., Haycock, J.W., 1995. Striatal 3,4-dihydroxyphenylalanine decarboxylase in aging: disparity between post-mortem and positron emission tomography studies? *Annals of Neurology* 38 (2), 260–264.
- Koepp, R.A., Mangner, T., Betz, A.L., Shulkin, B.L., Allen, R., Kollros, P., Kuhl, D.E., Agranoff, B.W., 1990. Use of [ $^{11}\text{C}$ ]aminocyclohexanecarboxylate for the measurement of amino acid uptake and distribution volume in human brain. *Journal of Cerebral Blood Flow and Metabolism* 10, 722–739.
- Kumakura, Y., Vernaleken, I., Grunder, G., Bartenstein, P., Gjedde, A., Cumming, P., 2005. PET studies of net blood–brain clearance of FDOPA to human brain: age-dependent decline of [ $^{18}\text{F}$ ]fluorodopamine storage capacity. *Journal of Cerebral Blood Flow and Metabolism* 25, 807–819.
- Kuwabara, H., Cumming, P., Reith, J., Leger, G., Diksic, M., Evan, A.C., Gjedde, A., 1993. Human striatal L-dopa decarboxylase activity estimated in vivo using 6-[ $^{18}\text{F}$ ]fluoro-dopa and positron emission tomography: error analysis and application to normal subjects. *Journal of Cerebral Blood Flow and Metabolism* 13, 43–56.
- Laakso, A., Vilkin, H., Bergman, J., Haaparanta, M., Solin, O., Syvalahti, E., Salokangas, R.K.R., Hietala, J., 2001. Sex differences in striatal presynaptic dopamine synthesis capacity in healthy subjects. *Biological Psychiatry* 52, 759–763.
- Lloyd, K.G., Hornykiewicz, O., 1972. Occurrence and distribution of aromatic L-amino acid (L-DOPA) decarboxylase in the human brain. *Journal of Neurochemistry* 19 (6), 1549–1559.
- Mai, J., Assheuer, J., Paxinos, G., 1997. *Atlas of the Human Brain*. Academic Press, New York.
- Markianos, M., Lykouras, L., 1981. Circadian rhythms of dopamine-beta-hydroxylase and c-AMP in plasma of controls and patients with affective disorders. *Journal of Neural Transmission* 50 (2–4), 149–155.
- Martin, W.R.W., Palmer, M.R., Patlak, C.S., Calne, D.B., 1989. Nigrostriatal function in man studies with positron emission tomography. *Annals of Neurology* 26, 535–542.
- Melega, W.P., Luxen, A., Perlmutter, M.M., Nissenson, C.H., Phelps, M.E., Barrio, J.R., 1990. Comparative in vivo metabolism of 6-[ $^{18}\text{F}$ ]fluoro-L-dopa and [ $^3\text{H}$ ]L-dopa in rats. *Biochemical Pharmacology* 39, 1853–1860.
- Oldendorf, W.H., 1971. Brain uptake of radiolabeled amino acids, amines, and hexoses after arterial injection. *American Journal of Physiology* 221, 1629–1639.
- Owen, A.M., James, M., Leigh, P.N., Summers, B.A., Marsden, C.D., Quinn, N.P., Lange, K.W., Robbins, T.W., 1992. Fronto-striatal cognitive deficits at different stages of Parkinson's disease. *Brain* 115 (Pt 6), 1727–1751.
- Patlak, C.S., Blasberg, R.G., 1985. Graphical evaluation of blood-to-brain transfer constants from multiple-time uptake data. Generalization. *Journal of Cerebral Blood Flow and Metabolism* 5, 584–590.
- Renkin, E.M., 1959. Transport of potassium-42 from blood to tissue in isolated mammalian skeletal muscles. *American Journal of Physiology* 197, 1205–1210.
- Sasaki, M., Ikemoto, M., Mutoh, M., Haradahira, T., Tanaka, A., Watanabe, Y., Suzuki, K., 2000. Automatic synthesis of L-[ $\beta$ - $^{11}\text{C}$ ] amino acids using an immobilized enzyme column. *Applied Radiation and Isotopes* 52 (2), 199–204.
- Sawle, G.V., Colebatch, J.G., Shah, A., Brooks, D.J., Marsden, C.D., Frackowiak, R.S.J., 1990. Striatal function in normal aging: implications for Parkinson's disease. *Annals of Neurology* 28, 799–804.
- Suhara, T., Fukuda, H., Inoue, O., Itoh, T., Suzuki, K., Yamasaki, T., Tateno, Y., 1991. Age-related changes in human D1 dopamine receptors measured by positron emission tomography. *Psychopharmacology (Berl)* 103, 41–45.
- Taki, Y., Goto, R., Evans, A., Zijdenbos, A., Neelin, P., Lerch, J., Sato, K., Ono, S., Kinomura, S., Nakagawa, M., Sugiura, M., Watanabe, J., Kawashima, R., Fukuda, H., 2004. Voxel-based morphometry of human brain with age and cerebrovascular risk factors. *Neurobiology of Aging* 25, 455–463.
- Taylor, S.F., Koepp, R.A., Tandon, R., Zubieta, J.K., Frey, K.A., 2000. In vivo measurement of the vesicular monoamine transporter in schizophrenia. *Neuropsychopharmacology* 23, 667–675.
- Tedroff, J., Aquilonius, S.M., Hartvig, P., Lundqvist, H., Bjurling, P., Langstrom, B., 1992. Estimation of regional cerebral utilization of [ $^{11}\text{C}$ ]-L-3,4-dihydroxy-phenylalanine (DOPA) in the primate by positron emission tomography. *Acta Neurologica Scandinavica* 85, 166–173.
- Torstenon, R., Hartvig, P., Langstrom, B., Westerberg, G., Tedroff, J., 1997. Differential effects of levodopa on dopaminergic function in early and advanced Parkinson's disease. *Annals of Neurology* 41 (3), 334–340.
- Torstenon, R., Tedroff, J., Hartvig, P., Fasth, K.J., Langstrom, B., 1999. A comparison of  $^{11}\text{C}$ -labelled L-DOPA and L-fluorodopa as positron emission tomography tracers for the presynaptic dopaminergic system. *Journal of Cerebral Blood Flow and Metabolism* 19, 1142–1149.
- Tupala, E., Hall, H., Bergstrom, K., Mantere, T., Rasanen, P., Sarkioja, T., Hiltunen, J., Tihonen, J., 2003. Different effect of age on dopamine transporters in the dorsal and ventral striatum of controls and alcoholics. *Synapse* 48, 205–211.
- Volkow, N.D., Ding, Y.S., Fowler, J.S., Wang, G.J., Logan, J., Gatley, S.J., Hitzemann, R., Smith, G., Fields, F., Gur, R., Wolf, A.P., 1996. Dopamine transporters decrease with age in healthy subjects. *Journal of Nuclear Medicine* 37, 554–558.
- Volkow, N.D., Gur, R.C., Wang, G.J., Fowler, J.S., Moberg, P.J., Ding, Y.S., Hitzemann, R., Smith, G., Logan, J., 1998. Association between decline in brain dopamine activity with age and cognitive and motor impairment in healthy individuals. *American Journal of Psychiatry* 155 (3), 344–349.
- Wade, L.A., Katzman, R., 1975. 3-O-methyldopa uptake and inhibition of L-DOPA at the blood–brain barrier. *Life Sciences* 17, 131–136.
- Wang, Y., Chan, G.L.Y., Holden, J.E., Dobko, T., Mak, E., Schulzer, M., Huser, J.M., Snow, B.J., Ruth, T.J., Calne, D.B., Stoessl, J., 1998. Age-dependent decline of dopamine D1 receptors in human brain: a PET study. *Synapse* 30, 56–62.

## A deficit in discriminating gaze direction in a case with right superior temporal gyrus lesion

Tomoko Akiyama\*, Motoichiro Kato, Taro Muramatsu, Fumie Saito, Ryoko Nakachi, Haruo Kashima

*Komagino Hospital, 273 Urataka-cho Hachioji City, Tokyo 193-8505, Japan*

Received 25 August 2004; received in revised form 22 April 2005; accepted 13 May 2005  
Available online 6 July 2005

### Abstract

The superior temporal sulcus (STS) region is well recognized as being heavily involved in detecting and discriminating gaze. Lesions confined to this area are quite rare in humans, and so the research has mainly depended on animal studies and functional neuroimaging in normal human subjects. We report one such rare case, a 54-year-old Japanese female with a possible congenital anomaly who, after a cerebral hemorrhage, demonstrated a lesion almost completely confined to the entire right superior temporal gyrus (STG). In the subacute phase, the patient showed evidence of left hemispatial neglect, from which she gradually recovered. In the chronic phase, she showed a puzzling difficulty in obtaining eye-contact. We have conducted, in conjunction with conventional neuropsychological evaluations, experimental assessment of her ability in gaze cognition. Her performance on neuropsychological testing demonstrated no compromise in intellect, memory, or language skills, and a close-to-full recovery from neglect. On gaze cognition experiments, she was repeatedly shown to perceive left gaze as straight, and to a lesser degree, straight gaze as right. We suggest that the function of the STG in detecting gaze, together with the directional information it receives from earlier visual areas, may be associated, when damaged, with this deficit in detecting contra-directional gaze. We have demonstrated for the first time that a single circumscribed lesion to the STG results in both gaze processing deficit and concurrent aberrant gaze behavior of the victim herself, implicating a mechanism within the STG as an interface between gaze of others and gaze of self. © 2005 Elsevier Ltd. All rights reserved.

**Keywords:** Superior temporal sulcus; Superior temporal gyrus; Gaze; Biological motion; Hemianopia

### 1. Introduction

The superior temporal sulcus (STS) has attracted much interest due to its intriguing function as a detector of biological motion. Since the 1980s, single-cell studies in monkey brains have shown that a number of neurons in the STS region show preference in the direction of head and gaze when viewing faces of conspecifics and humans, so that some neurons respond maximally to straight gaze while others respond more to averted gaze (Perrett, Hietanen, Oram, & Benson, 1992). Investigations of STS-lesioned monkeys showed disrupted gaze discrimination after lesioning (Campbell, Heywood, Cowey, Regard, & Landis,

1990; Eacott, Heywood, Gross, & Cowey, 1993), more or less supporting the findings from single-cell studies. Research of the STS in humans has found a homologous function; gaze as well as head direction, movement of mouth and hands, body gestures, geometric figures simulating biological motion have all been shown to activate the STS in functional imaging studies and electrophysiological studies (see Allison, Puce, & McCarthy, 2000; Puce & Perrett, 2003 for review). Thus, the function of the STS in humans can be summarized as the detection of biological motion, which composes a major contribution to social perception.

Gaze, in particular, is undoubtedly special, perhaps without a match in its significance as a biological signal. There are suggestions for the innateness of gaze cognition, in that newborns show a preference for faces with eyes open versus eyes closed (Batki, Baron-Cohen, Wheelwright, Connellan,

\* Corresponding author. Tel.: +81 426 63 2222; fax: +81 426 63 3286.  
E-mail address: tee-i@mxv.mesh.ne.jp (T. Akiyama).

& Ahluwalia, 2000), and that infants as early as 10 weeks of age follow the gaze of others (Hood, Willen, & Driver, 1998). Moreover, children as young as 4–5 years of age show much more organized ERPs (N190) to eyes compared to full faces (Taylor, Edmonds, McCarthy, & Allison, 2001a), implicating a system within the human brain which is dedicated, at least in part, to gaze cognition. Such a system has been suggested to be localized in the posterior region of the STS in question, particularly in the right hemisphere: In a PET study, faces with visible gaze compared with obscured gaze, was shown to differentially activate the STS (Wicker, Michel, Henaff, & Decety, 1998). Gaze processing, such as perception of apparent eye motion (Puce, Allison, Bentin, Gore, & McCarthy, 1998) and detection of gaze direction (Hoffman & Haxby, 2000), has also been demonstrated to elicit significant STS activation in fMRI studies. ERP studies have shown that N170 from the posterior temporal region is also sensitive to gaze (Puce, Smith, & Allison, 2000; Taylor, Itier, Allison, & Edmonds, 2001b).

Intriguing as it may be, however, the function of the STS in humans remains tentative in that most studies are based on functional findings of the intact brain. Neuropsychological studies of human cases with circumscribed STS lesions might be more conclusive, and would afford a wealth of insight into these issues. Since left STS damage would leave most humans aphasic with little understanding of any verbal input, study of a patient with right STS damage is likely to be more informative. To date, and to our knowledge, such a neuropsychological case has never been reported. In this paper, we report one such case, who, after a cerebrovascular accident, presented a very rare circumscribed lesion almost confined to the entire right superior temporal gyrus (STG), which constitutes the upper bank of the STS. The rarity of this lesion might have partly been due to a co-existing cerebrovascular anomaly in this patient. One of the most striking features of the sequelae in this patient was the inability to engage in mutual eye-contact. Given the functional data suggesting STS involvement in gaze cognition, a quantitative evaluation of the patient's gaze processing would offer the first neuropsychological data for the STS and its suggested role in gaze cognition. We have therefore conducted, in addition to conventional neuropsychological assessments, some behavioral experiments in gaze processing which revealed a unique impairment in gaze cognition.

## 2. Case description

The patient, M.J. is a right-handed, Japanese female with high school education who has been married for over 30 years and has successfully reared two children. She has no prior neurological or psychiatric history. At the time of onset, she was 54 years old. She presented with headache, nausea, slight left hemiparesis, and clouded consciousness. She was transferred to a nearby hospital, where her cranial CT revealed a

high density area in the right temporal lobe with a midline shift to the left, consistent with an acute cerebral hemorrhage. Cranial angiography revealed absence of the right internal carotid artery and depicted the left internal carotid artery feeding into the right middle cerebral artery region, pointing out a possible anomaly of the cranial arteries. Surgery was performed to remove the hematoma on the day of onset. After surgery, she quickly regained consciousness and her hemiparesis resolved within a course of a month. However, shortly after regaining consciousness, she complained of left-sided visual impairment. Upon visual field perimetry, a left homonymous hemianopia became evident. She also initially showed signs of left hemispatial neglect unexplainable with mere hemianopia, from which she gradually recovered within a course of a year. A puzzling behavior caught our attention after several sessions. When seated face to face with M.J., she often revealed a difficulty in obtaining eye-contact, with a tendency for M.J.'s gaze to drift to her contralateral, left. Her family confirmed that she has had no such difficulty prior to her cerebrovascular accident. On the other hand, she had no trouble fixating on objects when explicitly instructed to, as in the case where she was asked to look at the eyes of the observer. Thus, the drift in her gaze to the left was seen at rest, or during casual conversation, when M.J. was not keenly attending to any object.

The MRI in the chronic, stable phase demonstrated a rare, circumscribed lesion in the right STG, which slightly extended into the white matter underlying the gyrus (Fig. 1). The hemianopia can be explained by the lesion extension to the posterior horn of the lateral ventricle, thereby affecting the optic radiation. Also shown is a moderate atrophy of the right medial temporal structures compared to the intact left structures.

## 3. Neuropsychological assessment

Assessment was performed with conventional neuropsychological tests on two occasions (Table 1). The first assessment was administered 2–4 months after the onset of the hemorrhage when M.J. still had dense hemispatial neglect. The second assessment was delivered a year after the first, when the neglect had remitted. Between these two assessments, M.J. visited the outpatient department twice a month for non-structured rehabilitation.

### 3.1. Results

In the first assessment, M.J. performed within the normal range for intelligence, but showed a large discrepancy between verbal and visual material. Hemispatial neglect may explain most of the problem M.J. had on visual material, as can be seen in her performance for cancellation tests and line bisections. Detailed results are shown in Table 1.

In the second assessment, M.J. showed much improvement in many of the tests. The performance IQ in the WAIS-R

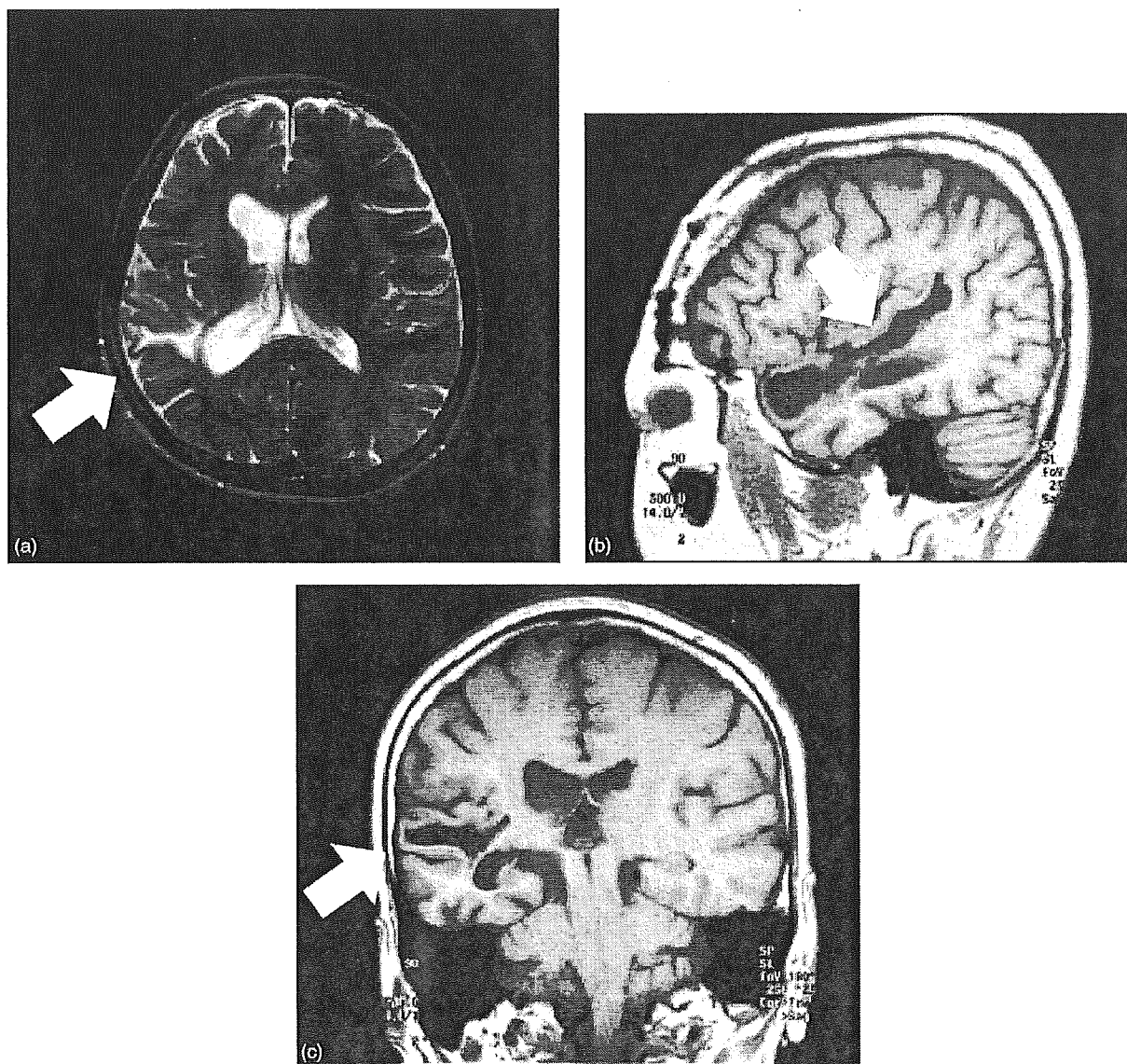


Fig. 1. MRI scan 2 years post onset. A rare lesion almost completely circumscribed to the entire STG, which is indicated by the arrows, is shown in the (a) axial, (b) sagittal, and (c) coronal slices. A moderate atrophy of the right medial temporal lobe can also be observed in the coronal slice.

was much better although there still remained a fair discrepancy between verbal IQ. Visual memory in the WMS-R also improved. On the cancellation test she omitted less. Her line bisections no longer deviated to the right, but now showed a minimal deviation to the left, which is not significantly deviant from pseudoneglect often demonstrated in normal subjects (Jewell & McCourt, 2000). Hemispatial neglect was assessed using the behavioral inattention test (BIT), a battery which has been validated and standardized in patients with stroke (Wilson, Cockburn, & Halligan, 1987a, 1987b). Her BIT score was well within the normal range, further indicating her recovery from the neglect syndrome. The performances on the Rey auditory verbal learning test were superior.

Overall, M.J.'s neuropsychological assessment showed that although she initially demonstrated signs of left hemispa-

tial neglect, it had nearly diminished within a course of a year. With this improvement, she presently shows no compromise in intellect, memory, or language skills.

#### 4. Experiment 1: gaze direction discrimination in digitized photographs

This and the following experimental investigations were carried out from the time of the second neuropsychological assessment, for a period of about a year. M.J. gave informed consent to participation in all experimental investigations. This study was approved by the ethical committee at our institutions. Note that all indications of 'right' and 'left' will refer to the direction from M.J.'s viewpoint. Note also that all

Table 1  
Neuropsychological scores

Test	First assessment	Second assessment
Wechsler adult intelligence scale—revised		
Verbal IQ	108	117
Performance IQ	87	101
Full IQ	99	111
Raven's coloured progressive matrices	32/36	34/36
Wechsler memory scale—revised		
Verbal memory	110	115
Visual memory	70	106
General memory	97	114
Delayed recall	93	107
Attention/concentration	98	101
Rey complex figure test		
Copy	36/36	33/36
Recall	20.5/36	15/36
Rey auditory verbal learning test		
Immediate recall	— <sup>a</sup>	10, 12, 14, 14, 15/15
Post-interference recall	—	15/15
Cancellation test		
Numerical 3	108/114 (95%), 133 s	113/114 (99%), 104 s
Japanese character 'ka'	99/114 (87%), 141 s	103/114 (90%), 130 s
Line bisection test (deviation as % total length)		
Midsagittal presentation	20.5% to right	4.5% to left
Right hemispace presentation	18.5% to right	5.0% to left
Left hemispace presentation	25.0% to right	5.5% to left
Behavioral inattention test		
Conventional subsets	—	144/146
Behavioral subsets	—	80/81

<sup>a</sup> Not administered.

materials were presented in her midsagittal plane, and that she was free to move her head and eyes during the tasks, unless stated otherwise.

A 77-year-old female patient with left homonymous hemianopia due to right thalamic hemorrhage (left hemianopic control, LH), a 43-year-old male with right homonymous hemianopia after left occipital lobe hemorrhage (right hemianopic control A, RH-A), and a 51-year-old male with right homonymous hemianopia due to traumatic brain injury of the optic radiation (right hemianopic control B, RH-B) served as hemianopic controls in all the experiments. Ten healthy adults (five males, five females, mean age 37.5) also participated in Experiments 1 and 3, and five from this group in Experiment 2, as normal subjects.

#### 4.1. Method

Three digitized photographs of a female looking straight at the camera (S), 8° to the right (R) and to the left (L) of the camera were taken. To control for any asymmetry of the face or the eyes, each picture was then reproduced with a

right/left inversion. A total of six photographs, i.e. S, R, L, S-inv, R-inv, and L-inv were obtained. The photographs were trimmed so that only the eye region, including the eyebrows, was shown (70 mm × 32 mm, Fig. 2a). In each photograph, the width of one eye measured approximately 16 mm, and the diameter of the iris 6 mm. Fifteen copies of each six photographs were made and placed in a pseudorandom order to make a set of 90 consecutive photographs of the eye region with three different gaze directions, and were shown singly on a 248 mm × 188 mm PC screen. The viewing distance was approximately 400 mm. M.J. was asked to report the direction of the gaze as right, left, or straight from her viewpoint. She was given unlimited time to respond, but all her responses were prompt, rarely taking more than 2 s.

#### 4.2. Results

M.J. discriminated the gaze direction correctly in 68 out of 90 photographs, giving her an error rate of 24.4%, which is substantially higher than that of the hemianopic controls (LH 14.4%, RH-A 1.1%, RH-B 7.8%), and normal controls (3.3%). Of the three directions, left gaze had the highest error rate for M.J., 40% of which were incorrectly perceived as straight gaze (Fig. 2b). As a contrast, LH misperceived right gaze as straight (76.9% of the errors were misperception of right gaze as straight, the remaining 23.1% were misperception of straight gaze as left), and RH-B made random errors without any directionality.

A  $\chi^2$  analysis was conducted to assess the differences in the distribution of error responses. M.J.'s error ratio was significantly higher than RH-A, RH-B and normal controls ( $p < 0.01$ ). No significant difference was observed between LH and normal controls ( $p = 0.24$ ). Although not reaching significance, M.J. showed a tendency to have more errors than LH ( $p = 0.09$ ) in addition to the opposite bias in the direction of errors (M.J., rightward; LH, leftward).

### 5. Experiment 2: mutual gaze detection

Given the suggestion that mutual gaze might be significant in its own right (George, Driver, & Dolan, 2001; Kampe, Frith, Dolan, & Frith, 2001; Kawashima et al., 1999), we wanted to test whether M.J. had preserved cognition of this fundamental aspect of gaze—the detection of mutual gaze. We realized that neither photographs nor videotapes would be a true equivalent of a real-life mutual gaze, so we designed this experiment with real-life gaze in a more natural setting.

#### 5.1. Method

An experimenter well acquainted with M.J. stood face to face with her, one meter away, with M.J. standing against a wall. On the wall behind M.J. and to both sides were 11 markers at the same height as M.J.'s eyes. The five markers closest to M.J. were 60 mm apart, and the remaining six

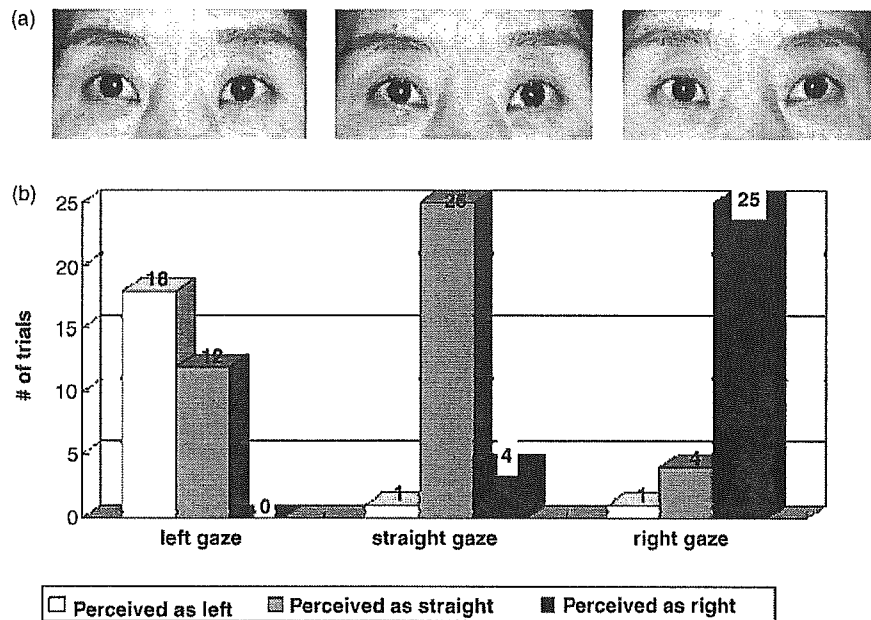


Fig. 2. (a) Examples of photographs used in Experiment 1. (b) Results of M.J.'s performance in Experiment 1. Gaze direction was discriminated in 90 digitized photographs (left gaze, 30; straight gaze, 30; right gaze, 30). M.J.'s performance is shown in relation to each gaze direction.

were 90 mm apart, comprising a gaze angle of approximately  $36^\circ$  for the farthest marker. The experimenter pursued each marker from either the extreme right or the left, alternating the starting point with each trial. Each target was viewed for approximately 1 s. When the experimenter's gaze reached the marker right next to M.J.'s face, the next marker was her nasal bridge, followed by the markers on the other side. M.J. was asked to look straight ahead at the experimenter's eyes during these trials, and to inform the experimenter when she felt their eyes met. M.J.'s eye-position was monitored by the observation of an independent experimenter to assure that she maintained straight gaze. The experiment consisted of 12 trials, and the closest marker being looked at when M.J. reported mutual gaze detection was recorded. The distance of these markers from M.J.'s nasal bridge was determined, then calculated into degrees of deviation from her nose.

## 5.2. Results

Throughout the experiment, M.J. did not show any difficulty following the instruction to look straight ahead. In the six trials where the pursuit began at M.J.'s extreme left, she was shown to perceive gaze looking slightly to the left of her face as mutual gaze, with an average deviation of  $11.1^\circ$  to the left. In other words, gaze slightly deviated to M.J.'s left was perceived as mutual, showing the same directionality in gaze misperception as seen in Experiment 1. On the other hand, M.J. was much more precise in detecting mutual gaze in the six trials where the pursuit began at her extreme right, with an average deviation of  $0^\circ$ . The average deviations for LH were  $0^\circ$  for trials beginning from the left, and  $7.0^\circ$  to the right for

trials beginning from the right. For RH-A and RH-B, and for all five normal control subjects, the average deviations were  $0^\circ$  and  $0^\circ$ , respectively, for either direction.

## 6. Experiment 3: direction discrimination in schematic eyes

To investigate whether the gaze discrimination impairment seen in Experiments 1 and 2 were gaze-specific, and not just a reflection of the residual spatial inattention per se, two types of schematic eyes (rectangular and elliptical) were designed and used as control tasks in direction discrimination.

### 6.1. Method

Rectangular schematic eyes consisted of rectangular diagrams in pairs. A black rectangle ( $6\text{ mm} \times 10\text{ mm}$ ) which was made to resemble the iris, was placed within a white rectangle ( $16\text{ mm} \times 10\text{ mm}$ ) resembling the sclera. The horizontal side of the black rectangle had a length matching the diameter of the iris in Experiment 1, and the white rectangle had a horizontal side matching the width of the eyes in Experiment 1. There were three orientations of the black rectangle in relation to the white; in the center (C), or slightly deviated to the right (R) or the left (L) of the center. The deviation was approximately 6.5% off the center relative to the entire horizontal length, which in effect was comparable to the right/left deviation of the gaze in Experiment 1. Two such identical diagrams were shown in pairs in a horizontal array (Fig. 3a).

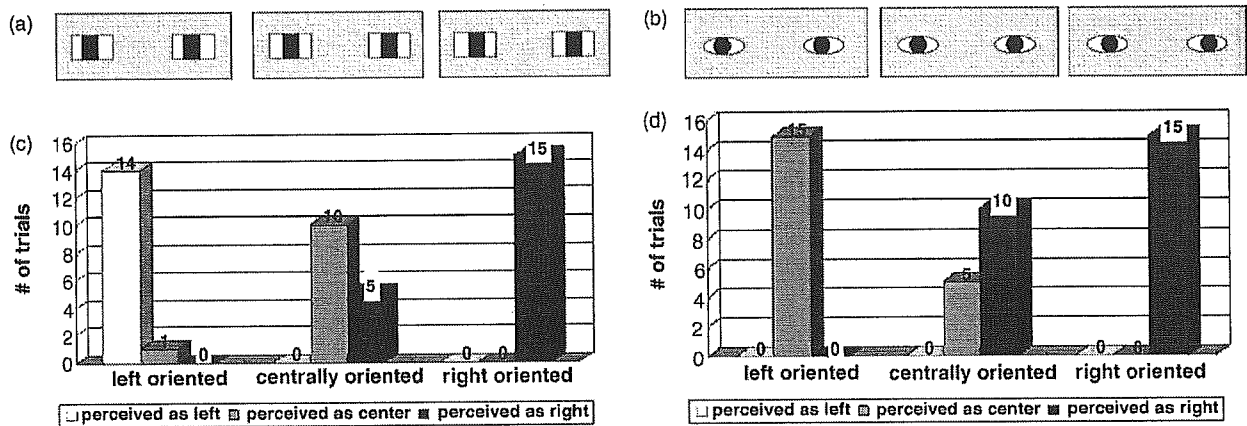


Fig. 3. Examples of (a) rectangular and (b) elliptical schematic eyes used in Experiment 3. Results of M.J.'s performance in (c) rectangular and (d) elliptical schematic eyes of Experiment 3. The direction of the schematic 'iris' was discriminated in 45 schematic eyes (left-oriented schema, 15; straight-oriented schema, 15; right-oriented schema, 15) for both configurations. M.J.'s performance is shown in relation to each 'gaze' orientation.

Fifteen copies of each orientation were made and placed in a pseudorandom order to make a set of 45 consecutive diagrams with three different orientations of the black 'iris', and were shown on the same PC screen.

Elliptical schematic eyes consisted of diagrams in pairs again, but this time with black circles (diameter: 6 mm) for the iris and white ellipses (axes: 16 mm  $\times$  10 mm) for the sclera. The size of the circles and ellipses were made to match the size of the iris and the eye in Experiment 1. The schematic iris was oriented either in the center (C) of the schematic sclera, or slightly deviated to the right (R) or the left (L) of the center, with comparable deviation as in Experiment 1 (approximately 6.5% off center), and were shown in pairs (Fig. 3b). These were also made into a set of 45 diagrams, and were shown on the PC screen. The viewing distance was approximately 400 mm. M.J. was asked, first for the rectangles, then for the ellipses, to report the orientation of the black figures in relation to the white, with right, left, or center from her viewpoint. Again, she was given unlimited time, but her responses were prompt. One thing of note is that the resemblance of these diagrams to eyes was never explicitly mentioned by the experimenter.

## 6.2. Results

For the rectangles, M.J. discriminated the orientation of the black 'iris' correctly in 39 out of 45, giving her an error rate of 13.3%, which was higher than that of the hemianopic controls (LH 4.4%, RH-A 8.9%, RH-B 0%), and substantially higher than that of normal controls (0.4%). In respect to each orientation in M.J.'s performance, none of the right-oriented rectangles were misjudged, but 33.3% and 6.7% of the centrally oriented (C), and left-oriented (L) rectangles were misjudged, respectively (Fig. 3c).

For the ellipses, M.J. discriminated the orientation correctly in 20 out of 45, giving her an error rate of 55.6%,

which contrasts sharply with the good performance for both control groups (LH 0%, RH-A 8.9%, RH-B 0%, normal controls 0.4%). A  $\chi^2$  analysis demonstrated that M.J.'s error ratio was significantly higher than LH, RH-A, RH-B, and normal controls ( $p < 0.01$ ). In respect to each orientation in M.J.'s performance, R ellipses were never misjudged, compared to the surprisingly high error rates of 66.7 and indeed, 100% for the C and L ellipses, respectively (Fig. 3d).

Most strikingly, all the errors that M.J. made reflected a directional bias to the right throughout both configurations; L diagrams had a strong tendency to be erroneously perceived as C, and C diagrams as R. RH-A also made systematic errors, albeit slighter, in the opposite direction; R diagrams were misjudged as C, and C diagrams as L. However, the error rates were identical between the two configurations. On the other hand, M.J. showed a much higher error rate for the ellipses compared to the rectangles, demonstrating a relative specificity of her impairment to stimuli which more closely resemble the eyes. It is worth mentioning that it was after the

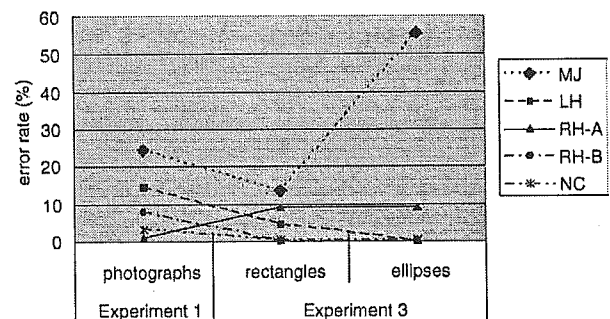


Fig. 4. Summary of the results for all participants in Experiment 1 (discriminating gaze direction from photographs of eyes) and Experiment 3 (discriminating 'gaze' direction from rectangular and elliptical schematic eyes) is shown as error rates for each stimulus type. x-axis, type of stimuli tested; y-axis, error rate in percentage. LH, left hemianopia; RH-A and B, right hemianopia; NC, normal control.

trial with the rectangles, and at the very beginning of the trial with the elliptical eyes that M.J. spontaneously became aware of the resemblance of the diagrams to eyes. Possibly with this awareness, the error rate of L and C diagrams significantly increased from 20.0% for the rectangles, to 83.3% for the ellipses. A conceptual rephrasing of this finding might be that when the diagrams were perceived, not as geometric diagrams but as schematic eyes, more than 80% of the left ‘gaze’ and straight ‘gaze’ were misjudged with a heavy directional bias to the right.

A summary of the results for Experiments 1 and 3 is shown in Fig. 4.

## 7. Discussion

M.J., who after a near-complete damage of the right STG in her fifth, heretofore uneventful decade, became longstandingly hemianopic, but recovered gradually from her initial left hemispatial neglect with some subtle residual impairments that were no longer detectable by conventional neuropsychological assessment. The most puzzling of these impairments was a difficulty in obtaining eye contact. Taken together the implication that the STS (the upper bank of which comprises the STG) is involved heavily in gaze detection, we were prompted to evaluate M.J.’s gaze cognition in detail. As has been shown, a unique directional impairment in gaze discrimination was demonstrated; M.J. was repeatedly shown to perceive left gaze as straight, and to a lesser degree, straight gaze as right in photographs (Experiment 1), in real encounters (Experiment 2), and in schematic eyes (Experiment 3). To the best of our knowledge, such impairment has never been reported in association with human brain damage. For the first time, then, has the repeated implication of STS involvement in gaze processing been supported neuropsychologically in humans.

### 7.1. The directional property of gaze

It actually does not come as too much of a surprise, given animal lesioning data (Campbell et al., 1990) and human functional data (Hoffman & Haxby, 2000; Pelphrey, Singerman, Allison, & McCarthy, 2003; Puce et al., 1998, 2000; Taylor et al., 2001b; Wicker et al., 1998), that a human lesion of the STS should also impair gaze cognition, as seen in this case. What came across as surprising, however, was the finding of a *directionality* (i.e., the consistent rightward bias) in M.J.’s perception of gaze, specifically when she currently demonstrates minimal if any signs of neglect in standardized testing. The impairment could be termed as a deficit in discriminating contralesional gaze direction. As such an impairment is quite novel, we believe it deserves further discussion.

There is growing body of research which elegantly demonstrates the automatic direction-cueing role of gaze. Friesen and Kingstone (1998) showed, in normal subjects, that targets

shown with schematic faces gazing in their direction elicited shorter detection time compared to targets with schema gazing in the opposite direction. Even more compelling are the findings that suggest that gaze, when compared to other non-biological directional cues, has a distinct directional valence of its own. Gaze, but not arrows, has been demonstrated to elicit gaze-following behavior in adults (Ricciardelli, Bricolo, Aglioti, & Chelazzi, 2002). Zorzi, Mapelli, Rusconi, and Umiltà (2003) have found that gaze direction has an effect independent from that cued by an egocentrically-defined directional signal, in behavioral tasks discriminating direction. In an fMRI study, Hooker et al. (2003) have demonstrated that direction-informing gaze differentially activates the STS, compared to arrows, non-directional eye motion, and even arrows superimposed on a photograph with uninformative gaze. Additional support for the involvement of the STS in detecting direction from gaze is offered by Pelphrey et al. (2003) who demonstrated a difference in MR signal waveform in the STS, between conditions where the schematic gaze oriented correctly or incorrectly in the direction of the target. These findings suggest three important points. Firstly, gaze has a definitive direction-cueing property. Secondly, gaze, in contrast to other directional cues, is in the position to differentially attract the gaze and attention of the viewer. Lastly, this directional information derived from gaze seems to be processed, at least to some extent, within the STS as shown in the last two fMRI studies.

How is the STS in the position to process such directional information? Two lines of evidence might be relevant to this question. A region termed the medial temporal/medial superior temporal cortex (MT/MST) in the monkey brain, which lies posterior to, and subsequently earlier in the visual stream than the STS, is recognized as a visual area tuned selectively to the direction of motion (see Wurtz, Yamasaki, Duffy, & Roy, 1990 for review). In humans, a group of unilateral brain-damaged subjects whose lesion overlapped in Brodmann area 19/37 were demonstrated to have a directional deficit in motion perception (Barton, Sharpe, & Raymond, 1995, 1996; Vaina, Cowey, Eskew, LeMay, & Kemper, 2001a) and smooth pursuit (Barton et al., 1996). This area at the temporo-parieto-occipital (TPO) junction, also activated in functional imaging studies tapping motion perception processing (Tootell et al., 1995; Watson et al., 1993), has since been considered the human homologue of MT/MST. The direction-sensitive information from the MT/MST is known to terminate at the superior temporal polysensory area in the STS of the monkey brain, which is precisely where the processing of biological motion, gaze being one of them, is implicated in humans (Bonda, Petrides, Ostry, & Evans, 1996; Vaina, Solomon, Chowdhury, Sinha, & Belliveau, 2001b). The second line of evidence comes from a report by Karnath, Ferber, and Himmelbach (2001), studying 25 human patients with hemispatial neglect, which revealed that the center of maximal lesion overlap among these patients was in the STG. This finding might lend additional support that there is indeed some directional processing in this gyrus. To summarize, the

STS (or the STG) in question is well in the position to receive directional information pertaining to the biological motion it processes. Accordingly, we have found for the first time, in a right STG-damaged case, a contra-directional impairment in one of the most robust biological motions; gaze. It does not go beyond speculation, but this finding might imply that leftward gaze is represented in the right STS (and perhaps rightward gaze in the left STS).

### 7.2. Influence of hemianopia

It has been shown, in hemianopics without neglect, that horizontal lines in the compromised visual field have a tendency to be overestimated, or perceived as longer than their true length, while lines in the intact field are underestimated, or perceived as shorter than their true length (Barton, Behrmann, & Black, 1998; Doricchi, Onida, & Guariglia, 2002). A good illustration of this tendency is shown in line bisections of such subjects, where the subjective midpoints fall into the contralesional half of the line. Normal subjects are also shown, when viewing lines only in their right visual field, to have a tendency to bisect them centripetally, or to the left, of the actual center (Nielsen, Intriligator, & Barton, 1999). These consistent findings may offer a completely different explanation for M.J.'s directional gaze impairment; as a left hemianopic, she over-represents the left side of the sclera, resulting in rightward misrepresentation of the iris. However, we argue against this interpretation as the sole mechanism for M.J.'s gaze processing deficit under the following grounds.

First of all, the left hemianopic control patient performed better than M.J. in all the experiments. More importantly, the error pattern that this control patient demonstrated in Experiments 1 and 2 was of a *leftward* bias, opposite to that of M.J. Although this control patient does not presently demonstrate robust left neglect, her performance on the BIT (Conventional subsets 133/146, Behavioral Subsets 74/81), though above the cutoff points, are worse than that of M.J. (144/146 and 80/81, respectively). This small difference might have affected this control patient's performance; the leftward bias that she demonstrated might have perhaps been a reflection of residual left neglect, i.e., the left side of the sclera is neglected, resulting in leftward misrepresentation of the iris. On the other hand, this left hemianopia control showed little compromise in Experiment 3, demonstrating clearly that the poor performance thereof on M.J.'s part cannot be explained by left hemianopia, nor left neglect for that matter. It is indeed difficult to disentangle left hemianopia from left neglect in right hemisphere damage (Daini, Angelelli, Antonucci, Cappa, & Vallar, 2002; Walker, Findlay, Young, & Welch, 1991), and in this sense, right hemianopia might control for a purer hemianopic effect unaffected by right hemispheric spatial impairment.

Turning, then, to the right hemianopic controls, both were essentially unimpaired in Experiments 1 and 2. It is true that in Experiment 3, one of the right hemianopic controls (RH-A) made substantial directional errors which might be

accounted for by his hemianopia, but the error rates remained constant between rectangular and elliptical configurations. It is worth emphasizing that none of the hemianopic controls, left or right, showed the quadruple increase in errors that M.J. demonstrated for elliptical, compared to rectangular eyes (Fig. 4). Thus, a mechanism independent from hemianopia, and specific to gaze, is called for. We conclude that, as much as a contribution of hemianopia might seem likely, as seen in the comparable error rates of M.J. and RH-A for the rectangular eyes, hemianopia also cannot explain M.J.'s core deficit in gaze processing. Instead, the involvement of the STG seems to have been essential in causing her impairment.

### 7.3. Your gaze, my gaze

One final observation will be discussed here; M.J.'s difficulty in engaging in mutual eye-contact, with a tendency of her gaze to drift to her contralesional left. Patients with injuries to the unilateral TPO junction are known to be impaired in pursuing targets with their eyes (Morrow & Sharpe, 1990, 1993; Thurston, Leigh, Crawford, Thompson, & Kennard, 1988). It is quite ecological that this smooth pursuit center should lie so closely together with the gaze processing region; it is advantageous for the gaze-following behavior so automatic (Ricciardelli et al., 2002), so essential (Baron-Cohen, 1995), and perhaps innate (Hood et al., 1998) to humans. It might well be said that intact gaze cognition is essential in developing normal gaze behavior like eye-contact and gaze-following. For example, autistic children, whose lack of reciprocal gaze exchange is one of the most striking manifestations, have been shown to demonstrate aberrant gaze processing (Senju, Tojo, Dairoku, & Hasegawa, 2004; Senju, Yaguchi, Tojo, & Hasegawa, 2003). Likewise, gaze processing impairment due to STG damage, as seen in this case, could also be speculated to hamper the gaze behavior of the victim herself.

Another potential interpretation might be that the leftward deviation in M.J.'s eye-position is in itself sufficient in explaining her rightward bias in gaze perception. We would like to point out, however, that M.J. was not observed to show any trouble fixating on the stimuli presented to her in Experiments 1 and 3, and was also able to maintain straight gaze when instructed to, in Experiment 2, as has been monitored by an independent observer. Additionally, had there been a mass effect of eye-position that the experimenters overlooked, the results for the rectangular and elliptical eyes in Experiment 3 should have been quite similar. Instead, a clear discrepancy is evident, favoring our hypothesis that the results seen in our experiments are a reflection of a deficit in gaze cognition, and not eye-position.

Most importantly, that the gaze processing of others should be impaired confluent with the gaze behavior of self, as an aftermath of a single circumscribed brain lesion is quite intriguing. One interpretation would be that these two phenomena are independent from each other and thus unrelated;

the leftward drift in her eye-position might be accounted for, not by her gaze processing deficit, but for example, by compensation for her left hemianopia. However, we have noted no difficulty in eye-contact, nor robust drift in eye-position in the three hemianopic control subjects. A larger control group might clarify the relationship between hemianopia and poor eye-contact. The second, and perhaps the more attractive interpretation might be that the two phenomena are indeed associated. If we were to imagine a window-like grid between two people facing each other, mutual gaze would be aligned with the midsagittal window. In the case of M.J., on the other hand, gaze looking through a window to M.J.'s left would be misperceived as mutual, and in an attempt to engage in mutual eye-contact herself, she might also direct her gaze in the direction of that left window. If we were to assume this position that the two phenomena are associated, it would be implicative of a mechanism in the STG which serves as an interface between the gaze of others and the gaze of self in its response. This neuropsychological case might be the first to demonstrate a neural ground for the intuition (and the substantial behavioral data), that your gaze is intimately associated with mine.

#### 7.4. Limitations

The limitations in this study leave some questions unanswered. Among them are: (1) Why does M.J. perform better for photographic eyes than schematic elliptical eyes, and why are the hemianopic control subjects inconsistent as to the stimuli he/she performs better, photographic or schematic? Normal control data suggest that the photographs are the more difficult stimuli (Fig. 4). For M.J., however, the photographs were worse than rectangular eyes, but better than elliptical eyes. The performances for RH-A also discord from normal data. A larger study with more control subjects and diverse stimuli might offer the answers. (2) Would M.J. show preserved or impaired attention-cueing effect of gaze (for example, Friesen & Kingstone, 1998; Kingstone, Tipper, Ristic, & Ngan, 2004), and what would her eye-movement pattern be like in such a paradigm? Basing on the data we have demonstrated in this study, we speculate that left gaze would be less effective than right gaze in orienting M.J.'s attention. We are hoping to explore into these issues in the future.

#### 8. Conclusions

This study has demonstrated, in a case with a rare right STG damage, a novel deficit in discriminating contralesional gaze direction. We have suggested that the function of the STG in processing gaze, together with the directional information it derives from earlier visual areas like the MT/MST, may be associated, when damaged, with such a deficit. Concurrent with this deficit was an impaired ability to obtain eye-contact, implicating that the STG might also serve as an

interface between the gaze of others, and gaze of self. As left hemispheric damage to the same region would obviously leave patients heavily aphasic, this rare case might serve as a prototype of human STG damage.

#### References

- Allison, T., Puce, A., & McCarthy, G. (2000). Social perception from visual cues: Role of the STS region. *Trends in Cognitive Sciences*, 4(7), 267–278.
- Baron-Cohen, S. (1995). *Mindblindness: An essay on autism and theory of mind*. Cambridge, MA: MIT Press.
- Barton, J. J., Behrmann, M., & Black, S. (1998). Ocular search during line bisection. The effects of hemi-neglect and hemianopia. *Brain*, 121(Pt 6), 1117–1131.
- Barton, J. J., Sharpe, J. A., & Raymond, J. E. (1995). Retinotopic and directional defects in motion discrimination in humans with cerebral lesions. *Annals of Neurology*, 37(5), 665–675.
- Barton, J. J., Sharpe, J. A., & Raymond, J. E. (1996). Directional defects in pursuit and motion perception in humans with unilateral cerebral lesions. *Brain*, 119(Pt 5), 1535–1550.
- Batki, A., Baron-Cohen, S., Wheelwright, S., Connellan, J., & Ahluwalia, J. (2000). Is there an innate gaze module? Evidence from human neonates. *Infant Behavior and Development*, 23, 223–229.
- Bonda, E., Petrides, M., Ostry, D., & Evans, A. (1996). Specific involvement of human parietal systems and the amygdala in the perception of biological motion. *Journal of Neuroscience*, 16(11), 3737–3744.
- Campbell, R., Heywood, C. A., Cowey, A., Regard, M., & Landis, T. (1990). Sensitivity to eye gaze in prosopagnosic patients and monkeys with superior temporal sulcus ablation. *Neuropsychologia*, 28(11), 1123–1142.
- Daini, R., Angelelli, P., Antonucci, G., Cappa, S. F., & Vallar, G. (2002). Exploring the syndrome of spatial unilateral neglect through an illusion of length. *Experimental Brain Research*, 144(2), 224–237.
- Doricchi, F., Onida, A., & Guariglia, P. (2002). Horizontal space misrepresentation in unilateral brain damage. II. Eye-head centered modulation of visual misrepresentation in hemianopia without neglect. *Neuropsychologia*, 40(8), 1118–1128.
- Eacott, M. J., Heywood, C. A., Gross, C. G., & Cowey, A. (1993). Visual discrimination impairments following lesions of the superior temporal sulcus are not specific for facial stimuli. *Neuropsychologia*, 31(6), 609–619.
- Friesen, C., & Kingstone, A. (1998). The eyes have it! Reflexive orienting is triggered by nonpredictive gaze. *Psychonomic Bulletin and Review*, 5(3), 490–495.
- George, N., Driver, J., & Dolan, R. J. (2001). Seen gaze-direction modulates fusiform activity and its coupling with other brain areas during face processing. *Neuroimage*, 13(6 Pt 1), 1102–1112.
- Grossman, E., Donnelly, M., Price, R., Pickens, D., Morgan, V., Neighbor, G., et al. (2000). Brain areas involved in perception of biological motion. *Journal of Cognitive Neuroscience*, 12(5), 711–720.
- Hoffman, E. A., & Haxby, J. V. (2000). Distinct representations of eye gaze and identity in the distributed human neural system for face perception. *Nature Neuroscience*, 3(1), 80–84.
- Hood, B. M., Willen, J. D., & Driver, J. (1998). Adult's eyes trigger shifts of visual attention in human infants. *Psychological Science*, 9, 53–56.
- Hooker, C. I., Paller, K. A., Gitelman, D. R., Parrish, T. B., Mesulam, M. M., & Reber, P. J. (2003). Brain networks for analyzing eye gaze. *Brain Research: Cognitive Brain Research*, 17(2), 406–418.
- Jewell, G., & McCourt, M. E. (2000). Pseudoneglect: A review and meta-analysis of performance factors in line bisection tasks. *Neuropsychologia*, 38(1), 93–110.
- Kampe, K. K., Frith, C. D., Dolan, R. J., & Frith, U. (2001). Reward value of attractiveness and gaze. *Nature*, 413(6856), 589.

- Karnath, H. O., Ferber, S., & Himmelbach, M. (2001). Spatial awareness is a function of the temporal not the posterior parietal lobe. *Nature*, *411*(6840), 950–953.
- Kawashima, R., Sugiura, M., Kato, T., Nakamura, A., Hatano, K., Ito, K., et al. (1999). The human amygdala plays an important role in gaze monitoring. A PET study. *Brain*, *122*(Pt 4), 779–783.
- Kingstone, A., Tipper, C., Ristic, J., & Ngan, E. (2004). The eyes have it!: An fMRI investigation. *Brain and Cognition*, *55*(2), 269–271.
- Morrow, M. J., & Sharpe, J. A. (1990). Cerebral hemispheric localization of smooth pursuit asymmetry. *Neurology*, *40*(2), 284–292.
- Morrow, M. J., & Sharpe, J. A. (1993). Retinotopic and directional deficits of smooth pursuit initiation after posterior cerebral hemispheric lesions. *Neurology*, *43*(3 Pt 1), 595–603.
- Nielsen, K. E., Intriligator, J., & Barton, J. J. (1999). Spatial representation in the normal visual field: A study of hemifield line bisection. *Neuropsychologia*, *37*(3), 267–277.
- Peiphrey, K. A., Singerman, J. D., Allison, T., & McCarthy, G. (2003). Brain activation evoked by perception of gaze shifts: The influence of context. *Neuropsychologia*, *41*(2), 156–170.
- Perrett, D. I., Hietanen, J. K., Oram, M. W., & Benson, P. J. (1992). Organization and functions of cells responsive to faces in the temporal cortex. *Philosophical Transactions of the Royal Society of London Series B: Biological Sciences*, *335*(1273), 23–30.
- Puce, A., Allison, T., Bentin, S., Gore, J. C., & McCarthy, G. (1998). Temporal cortex activation in humans viewing eye and mouth movements. *Journal of Neuroscience*, *18*(6), 2188–2199.
- Puce, A., & Perrett, D. (2003). Electrophysiology and brain imaging of biological motion. *Philosophical Transactions of the Royal Society of London Series B: Biological Sciences*, *358*(1431), 435–445.
- Puce, A., Smith, A., & Allison, T. (2000). ERPs evoked by viewing facial movements. *Cognitive Neuropsychology*, *17*, 221–239.
- Ricciardelli, P., Bricolo, E., Aglioti, S. M., & Chelazzi, L. (2002). My eyes want to look where your eyes are looking: Exploring the tendency to imitate another individual's gaze. *Neuroreport*, *13*(17), 2259–2264.
- Senju, A., Tojo, Y., Dairoku, H., & Hasegawa, T. (2004). Reflexive orienting in response to eye gaze and an arrow in children with and without autism. *Journal of Child Psychology and Psychiatry*, *45*(3), 445–458.
- Senju, A., Yaguchi, K., Tojo, Y., & Hasegawa, T. (2003). Eye contact does not facilitate detection in children with autism. *Cognition*, *89*(1), B43–B51.
- Taylor, M. J., Edmonds, G. E., McCarthy, G., & Allison, T. (2001). Eyes first! Eye processing develops before face processing in children. *Neuroreport*, *12*(8), 1671–1676.
- Taylor, M. J., Itier, R. J., Allison, T., & Edmonds, G. E. (2001). Direction of gaze effects on early face processing: Eyes-only versus full faces. *Brain Research: Cognitive Brain Research*, *10*(3), 333–340.
- Thurston, S. E., Leigh, R. J., Crawford, T., Thompson, A., & Kennard, C. (1988). Two distinct deficits of visual tracking caused by unilateral lesions of cerebral cortex in humans. *Annals of Neurology*, *23*(3), 266–273.
- Tootell, R. B., Reppas, J. B., Kwong, K. K., Malach, R., Born, R. T., Brady, T. J., et al. (1995). Functional analysis of human MT and related visual cortical areas using magnetic resonance imaging. *Journal of Neuroscience*, *15*(4), 3215–3230.
- Vaina, L. M., Cowey, A., Eskew, R. T., Jr., LeMay, M., & Kemper, T. (2001). Regional cerebral correlates of global motion perception: Evidence from unilateral cerebral brain damage. *Brain*, *124*(Pt 2), 310–321.
- Vaina, L. M., Solomon, J., Chowdhury, S., Sinha, P., & Belliveau, J. W. (2001). Functional neuroanatomy of biological motion perception in humans. *Proceedings of the National Academy of Sciences of the United States of America*, *98*(20), 11656–11661.
- Walker, R., Findlay, J. M., Young, A. W., & Welch, J. (1991). Disentangling neglect and hemianopia. *Neuropsychologia*, *29*(10), 1019–1027.
- Watson, J. D., Myers, R., Frackowiak, R. S., Hajnal, J. V., Woods, R. P., Mazziotta, J. C., et al. (1993). Area V5 of the human brain: Evidence from a combined study using positron emission tomography and magnetic resonance imaging. *Cerebral Cortex*, *3*(2), 79–94.
- Wicker, B., Michel, F., Henaff, M. A., & Decety, J. (1998). Brain regions involved in the perception of gaze: A PET study. *Neuroimage*, *8*(2), 221–227.
- Wilson, B., Cockburn, J., & Halligan, P. (1987a). *Behavioural inattention test*. Titchfield, Hampshire: Thames Valley Test Company.
- Wilson, B., Cockburn, J., & Halligan, P. (1987b). Development of a behavioral test of visuospatial neglect. *Archives of Physical Medicine and Rehabilitation*, *68*(2), 98–102.
- Wurtz, R. H., Yamasaki, D. S., Duffy, C. J., & Roy, J. P. (1990). Functional specialization for visual motion processing in primate cerebral cortex. *Cold Spring Harbor Symposia on Quantitative Biology*, *55*, 717–727.
- Zorzi, M., Mapelli, D., Rusconi, E., & Umiltà, C. (2003). Automatic spatial coding of perceived gaze direction is revealed by the Simon effect. *Psychonomic Bulletin and Review*, *10*(2), 423–429.



Case report

## Cortical reorganization and somatic delusional psychosis: A magnetoencephalographic study

Yutaka Kato<sup>a,b,e,\*</sup>, Taro Muramatsu<sup>a</sup>, Motoichiro Kato<sup>a,b</sup>, Yoshiyuki Shibukawa<sup>b,c</sup>,  
Masuro Shintani<sup>b</sup>, Fumihiko Yoshino<sup>b,d</sup>

<sup>a</sup> Department of Neuropsychiatry, School of Medicine, Keio University, Shinanomachi, Shinjuku-ku, Tokyo 160-8582, Japan

<sup>b</sup> Laboratory of Brain Research, Oral Health Science Center, Tokyo Dental College, Chiba 261-8502, Japan

<sup>c</sup> Department of Physiology, Tokyo Dental College, Chiba 261-8502, Japan

<sup>d</sup> Department of Neuropsychiatry, Tokyo Dental College Ichikawa General Hospital, Chiba 272-8513, Japan

<sup>e</sup> Inogashira Hospital, Tokyo 181-8531, Japan

Received 14 November 2004; received in revised form 31 March 2005; accepted 3 October 2005

### Abstract

A woman complained of feeling a “metal-like thing” in her oral cavity 4 years after a stroke. She was convinced of the physical nature of her complaint despite intact dental and neurological findings. Somatosensory evoked magnetic fields suggested that her decreased right SII function was compensated for by the right SI region, probably contributing to the delusional symptom. © 2005 Elsevier Ireland Ltd. All rights reserved.

**Keywords:** Magnetoencephalography (MEG); Somatosensory cortex; Psychopathology

### 1. Introduction

Behavioural syndromes similar to idiopathic psychiatric syndromes may occur after a brain insult such as a stroke. From a neuropsychological perspective, the lesion site should determine many characteristics of the behavioral alterations, and the lesion-deficit model has been used to attribute various cognitive functions to specific cortical regions. Aphasias as deficit symptoms of Broca's or Wernicke's areas represent classic examples. Other models involve the disconnection syndrome (Geschwind, 1965).

In the last decade evidence has emerged that the injured brain often undergoes significant ‘remodeling’ (Rauschecker, 1995). However, studies examining complex behavioral alterations following stroke have not been reported.

Herein we present a magnetoencephalographic (MEG) study of a woman who complained of “a metal-like thing” in her oral cavity 4 years after brain infarction. Somatosensory evoked magnetic fields (SEFs) suggested the contribution of post-stroke functional reorganization to the psychopathology.

### 2. Method

#### 2.1. Case report

U.O. was a 64-year-old woman who had no history of psychiatric illness. She suffered a right caudate

\* Corresponding author. Department of Neuropsychiatry, Keio University School of Medicine, 35 Shinanomachi, Shinjuku-ku, Tokyo 160-8582, Japan. Tel.: +81 3 3353 1211x62454; fax: +81 3 5379 0187.

E-mail address: [yutaka-k@db3.so-net.ne.jp](mailto:yutaka-k@db3.so-net.ne.jp) (Y. Kato).

stroke in 1994, but no neurological signs were noted. In 1998, she underwent surgery for periodontal disease, immediately after which she began complaining of “a metal-like thing” in her oral cavity, which was located near the left mandibular premolars. Repeated dental examinations revealed no abnormalities, but she was convinced of the physical nature of her complaint. She was referred to the psychiatric division in 2001, and prescribed medications, including neuroleptics, had no effect on her preoccupation.

## 2.2. MEG procedures

SEFs were examined for U.O. and for a control patient—H.J., who had suffered a bilateral caudate infarction but had no psychiatric symptoms. Both patients were right-handed and showed no neurological signs. They provided written informed consent, and the protocol was approved by the local ethics committee. Cortical magnetic signals were recorded with a 306-channel neuromagnetometer (Elekta Neuromag Oy, Helsinki, Finland) with a helmet-shaped array. The recording bandpass was 0.3–200 Hz, and the sampling rate was 600 Hz. Epochs with signals exceeding 1500 fT/cm were excluded from averaging. A total of 200 stimulations to each site were collected with an analysis period of 350 ms, including a pre-stimulus DC baseline of 50 ms. The exact position of the head was determined by coils with cranial landmarks using an Isotrak 3D digitizer (Polhemus, Colchester, VT).

## 2.3. Stimuli and device

SEFs were recorded from the patients by stimulating the following four sites: median nerves (right, left) and mental nerves (right, left). Electrical stimuli were delivered using an SEM-4201 electrical stimulator (Nihon Kohden Inc., Tokyo, Japan) with a 0.3-ms duration and an inter-stimulus interval of 3 s. The current intensity was twice the sensory threshold level and was below the individually determined pain threshold.

## 2.4. Data analysis

Cerebral sources of responses were modeled as equivalent current dipoles (ECDs), which were estimated using a spherical head model (Hamalainen et al., 1993). The ECDs that best described the predominant source were first determined by a least-squares search at response peaks. They were then extended to the entire time period and all channels. All ECDs were included simultaneously in the time-varying multi-dipole model

(Uusitalo and Ilmoniemi, 1997). The validity of the multi-dipole model was evaluated by comparing measured signals with responses predicted by the model, and good agreement was required for the model to be accepted.

## 3. Results

After somatosensory stimulation at the four sites, U.O. showed abnormalities at longer latencies. Conversely, the control patient (H.J.) displayed a normal SEF pattern, which was adequately explained by the three-dipole model.

### 3.1. Responses to right median nerve stimuli

ECDs of early (23.4 ms) and late (82.3 ms) components were clearly identified on the left hemisphere in U.O. Both ECDs were integrated to the postcentral wall of the central fissure (early) and the upper bank of the Sylvian fissure in the left parietal operculum (late), locations that were consistent with area 3b of SI and SII (Hari et al., 1983; Kakigi, 1994). However, the late component on the right hemisphere was completely silent in U.O., while the right late component was observed in the control patient H.J. (Fig. 1).

### 3.2. Responses to left median nerve stimuli

At latencies around 25 ms, ECDs were estimated on the right SI cortex in both subjects. For the late component, bilateral ECDs were also estimated at a latency of around 90 ms in both subjects. In U.O., no responses were observed from the right SII, and the right late component was identified near the right SI. This magnetic response was different from the late component observed in the posterior parietal cortex (PPC) and the medial frontal cortex (M source) in the latencies and distributions (Forss et al., 1996). The right late component in H.J. was localized to SII. The left SII showed normal activation in both patients. Source strengths suggested that these are activated independently (Fig. 2).

### 3.3. Responses to right foramen mentale stimuli

In U.O., both early and late components on the left hemisphere were represented by ECDs estimated in SI and SII. But the right SII did not properly activate compared with the response from control H.J., indicating functional disruption of the right SII in U.O.

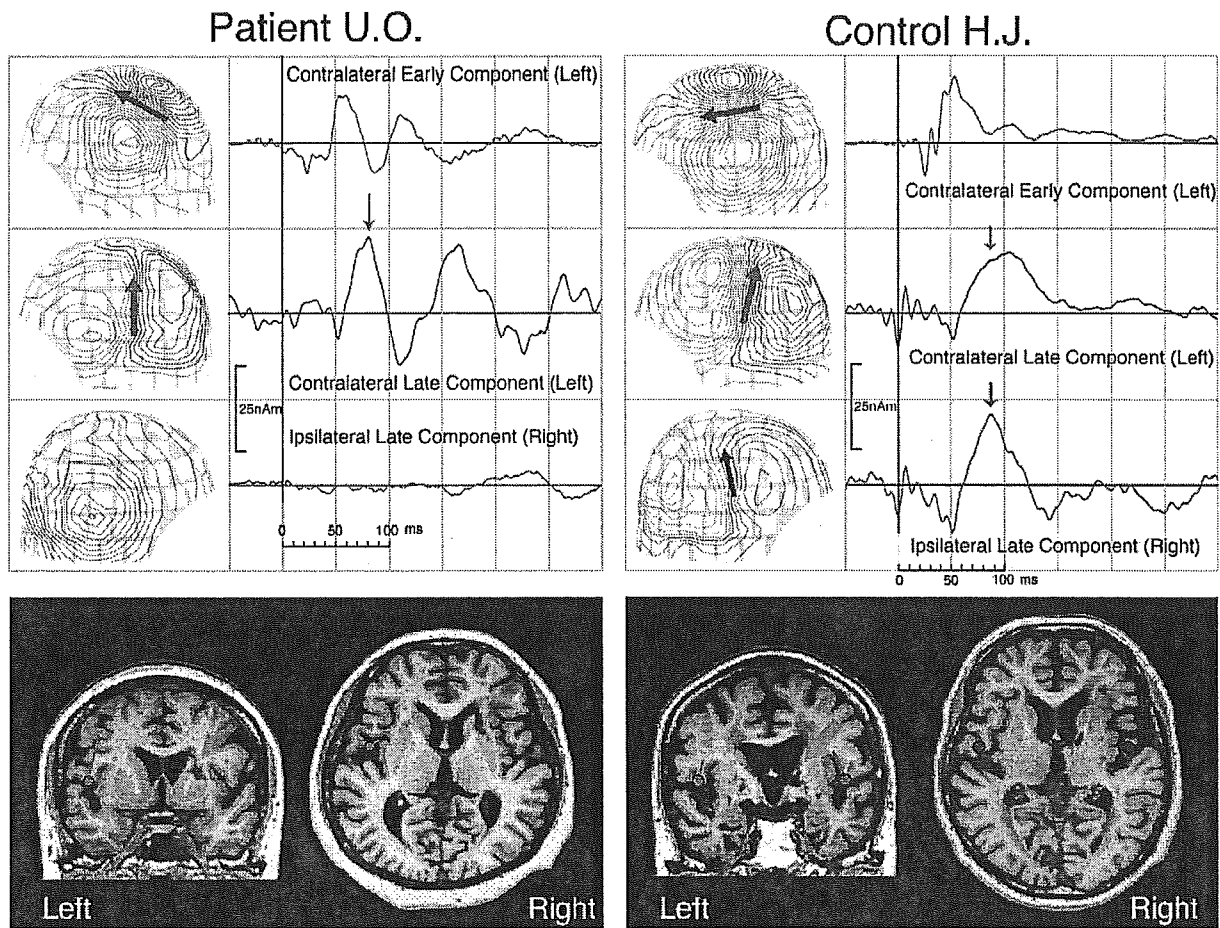


Fig. 1. Source strengths and MEG-MRI integrations of ECDs estimated by right median nerve stimuli. Patient U.O. (left panels), who suffered from a somatic delusion, displayed two components in the contralateral hemisphere, whereas control patient H.J. (right panels) exhibited three components in both hemispheres. Source strengths of contralateral early components are shown as a green line, contralateral late components (left hemisphere) as blue, and ipsilateral late components (right hemisphere) as red (in patient U.O., the ipsilateral late component was silent). Right contour maps were drawn over the left-side scalp surface (contralateral early and late components) and over the right-side scalp surface (ipsilateral late component) at peak latencies in each subject (82.3 ms in patient U.O., 91.2 ms in control H.J.). The lower panels show T1-weighted MRI for subjects displaying a small infarction in the right caudate nucleus (orange arrow). This panel also indicates MEG-MRI integrations of late components as a blue score for contralateral late components (left) and a red score for ipsilateral late components (right). The ipsilateral SII region was functionally disrupted in patient U.O. by stimulation to the right side of the body.

### 3.4. Responses to left foramen mentale stimuli

Through stimulation of the left mental nerve, where the subject actually experienced the “metal-like thing,” three ECDs were estimated corresponding to one early and two bilateral components in both subjects. All ECDs in control (H.J.) and two ECDs in U.O. were present in the proper regions. However, the contralateral late component was observed from the right SI in U.O., which might have resulted in confusion between early and late somatosensory processing. Since we could not observe any response from the right SII at longer latencies, the right SI might have compensated for right SII functionally.

### 4. Discussion

In neuromagnetic recordings, electric stimulation of peripheral nerves activates an extended cortical network, with the first responses in the contralateral SI. Later activity is seen bilaterally, usually more strongly on the left than the right in normal controls (Wegner et al., 2000), in the upper bank of the Sylvian fissure corresponding to the SII region (Hari et al., 1983). Because SII is activated by both ipsilateral and contralateral stimuli, it might be involved in bilateral somatosensory integration (Simoes et al., 2002) and thus considered to be involved in the integration of tactile stimuli by comparing actual